

# Ferromagnetic Ordering in Carbon Nanotubes, Incorporated in Diamond Single Crystals

Dmitri Yerchuck (a), Vyacheslav Stelmakh (b), Alla Dovlatova (c), Yauhen Yerchak (b), Andrey Alexandrov (c)  
(a) - Heat-Mass Transfer Institute of National Academy of Sciences of RB, Brovka Str., 15, Minsk, 220072, RB,  
dpy@tut.by

(b) Belarusian State University, Nezavisimosti Avenue 4, Minsk, 220030,  
RB (c) - M.V.Lomonosov Moscow State University, Moscow, 119899

(Dated: November 17, 2018)

The physical origin of the mechanism of the formation of ferromagnetic ordering in carbon nanotubes (NTs), produced by high energy ion beam modification of diamond single crystals in  $\langle 110 \rangle$  and  $\langle 111 \rangle$  directions has been found. It is concluded from analysis of experimental results on ferromagnetic spin wave resonance observed, that the only  $\pi$ -electronic subsystem of given NTs is responsible for the appearance of ferromagnetism. It is determined by asymmetry in spin density distribution in Su-Schrieffer-Heeger (SSH) topological soliton lattice. The formation of SSH topological soliton lattice is considered in the frames of generalized SSH-model of organic conductors, in which  $\pi$ -electronic subsystem is represented being to be 1D quantum Fermi liquid.

PACS numbers: 71.10.-w, 73.63.Fg, 78.30.-j, 76.30.-v, 76.50.+g, 78.67.-n

Keywords: Ferromagnetism, Carbon, Nanotubes, Spin Wave Resonance, Quantum Fermi Liquid

## I. INTRODUCTION AND BACKGROUND

It is well known that all substances on the whole are magnetics. At the same time, it is also well known, that classical magnetic ordering is existing in the substances, which are built from the atoms with unfilled inner atomic  $d$ - or  $f$ -shells or include given atoms in their elementary units. In other words, classical magnetics are the substances, elementary units of which include transition chemical elements with unfilled atomic 3d-, 4d-, 5d-, 6d-shells, or rare earth elements with unfilled atomic 4f, 5f-shells. Carbon does not refer to given group. Nevertheless, there are at present a number of communications on magnetic ordering in carbon and carbon based materials.

The first report on the experimental revealing of magnetic ordering in carbon structurally ordered systems was presented on the IBMM-Conference in Knoxville, TN, USA [1] in 1990. Given result was confirmed in report on E-MRS Conference in Strasbourg, France [2] also in 1990. Let us remark, that the first report on magnetic ordering in structurally non-ordered carbon materials appeared almost in the same time. It is the work [3], where ferromagnetic ordering in pyrolytic carbon, produced by chemical vapour deposition (CVD) method using adamantane to be source material, was found. Let us also remark, that simultaneously, the reports [1], [2] were the first reports on the formation by high energy ion beam modification (HEIBM) of diamond single crystals structurally and magnetically ordered quasi-one-dimensional (quasi-1D) system along ion tracks, that is new carbon allotropic form, which was identified with nanotubes NTs, incorporated in diamond matrix in direction, precisely coinciding with ion beam direction. Given system possesses by a number of interesting physical properties, reported in [4], [5], [6], [7]. When concerne the magnetic ordering, it was established from the

study of temperature dependence of electron spin resonance (ESR) absorption intensity, that, for instance, incorporated nanotubes, produced by neon HEIBM of diamond single crystal along  $\langle 100 \rangle$  crystallographic direction, possess by weak antiferromagnetic ordering [4], [6], [7]. At the same time, copper HEIBM with implantation direction along  $\langle 111 \rangle$  crystal axis, nickel HEIBM with implantation direction along  $\langle 110 \rangle$  axis, [4], [6], [7], and boron HEIBM of polycrystalline diamond films with implantation direction transversely to film surface, [5], lead to formation of NTs, incorporated in diamond matrix, which are possessed by ferromagnetic ordering. It was established directly by observation of ferromagnetic spin wave resonance (FMSWR) [5], [6], [7]. The first observations of FMSWR in carbon materials and in the materials, which are non-traditional magnetic materials, on the whole, were reported in above cited works. It was established, that magnetic ordering is inherent property for carbon electronic system, that is, it is not connected with presence of magnetic impurities, since starting samples were selected in that way, that the absolute spin number of paramagnetic impurities and paramagnetic structural imperfections at all did not exceed the value  $10^{12}$  spins.

Very recently, [8], antiferroelectric ordering has been found in the same pure carbon allotropic form - quasi-1D carbon zigzag-shaped nanotubes (CZSNTs), obtained by boron- and copper-HEIBM of diamond single crystals in  $\langle 111 \rangle$ -direction. It was established by means of the detection of new optical phenomenon - antiferroelectric spin wave resonance (AFESWR), which was theoretically described and experimentally confirmed for the first time by infrared (IR) spectroscopy study of carbynes in [9]. It seems to be very new property of pure carbon allotropic forms - quasi-1D CZSNTs and carbynes. Moreover, on the observation of antiferroelectric ordering has been reported in [9] for the first time for all carbon and carbon

based systems on the whole. Given results mean, that pure carbon in the form of quasi-1D CZSNTs or carbynes is multiferroic system. Especially significant was the observation of AFESWR with linear  $k$ -dispersion law, where  $k$  is magnitude of wave vector  $\vec{k}$ . It was the first work, in which the general spin wave theory was experimentally confirmed. Let us remark, that given theory was starting from the work [10] in 1936 and was developed in many subsequent works, for instance, in [11], [12], [13], [14], [15], [16], however for antiferromagnetic spin wave case. At the same time, it has been shown in [9], that the conclusions of the antiferroelectric spin wave theory and antiferromagnetic spin wave theory are qualitatively identical, in particular, dispersion law is the same.

Let us also remark, that experimental observation of multiferroicity in quasi-1D CZSNTs and carbynes means the breakdown of space inversion symmetry along CZSNT hypercomplex symmetry axis and respectively along carbyne chain symmetry axis. In the case of CZSNTs, it agrees well with the model of quasi-1D CZSNTs [17], [8], based on bond dimerization in all chain components of quasi-1D CZSNT along its hypercomplex symmetry axis  $z$ , which actually leads to inversion symmetry breakdown along given axis. Therefore, the experimental observation of antiferroelectricity of quasi-1D CZSNTs, necessary condition for which is the evident prediction of the model (appearance of nonzero polarisation by atomic displacements), proposed in [17], can be considered to be additional argument in favour of given theoretical model. The idea of the formation of ferromagnetic ordering (or ferroelectric ordering) in quasi-1D carbon systems was proposed in [9]. It has been shown, that by asymmetric deviation of spin density relatively the chain direction the constant component is appeared. It can lead in the case of density wave formation along 1D axis to ferromagnetic ordering, if density wave distribution is magnetic spin distribution and to ferroelectric ordering by electric own moments or electric dipole distribution. At the same time, which subsystem (or subsystems), that is  $\pi$  subsystem or  $\sigma$  subsystem (or even both subsystems) is (are) responsible for ferromagnetic ordering in quasi-1D CZSNT was not established.

The aim of given work is to study in more details the properties of cylindrical nanotubes, produced in diamond single crystals by high energy ion implantation, which are possessing by  $C_\infty$  symmetry axis, and to experimentally establish the mechanisms of formation of ferromagnetic and ferroelectric ordering in given NTs.

## II. EXPERIMENTAL TECHNIQUE

Samples of type IIa natural diamond, implanted by high energy ions of nickel (the energy of ions in ion beam was 335 MeV, ion beam dose was  $5 \times 10^{14} \text{ cm}^{-2}$ ) and implanted by high energy ions of copper and boron (the energy of ions in ion beam was 63 MeV and 13.6 MeV for copper and boron ions correspondingly, ion beam dose

was  $5 \times 10^{14} \text{ cm}^{-2}$ ) have been studied. Nickel implanted sample was representing rectangle with the sides  $\approx 5$  and 4 mm in based (110) plane. Copper and boron implanted samples were representing in their geometry prisms with quilateral triangle in their bases, coinciding with (111) crystallographic plane, side of base triangle was equal to  $\approx 5$  mm. Thickness of all samples was equal to  $\approx 1$  mm. Ion implantation of copper and boron was performed along [111] crystal direction, that is transversely to triangle prism base uniformly along all the surface. Nickel implantation was performed along [110] crystal direction, that is transversely to based (110) rectangle plane also uniformly along all the plane surface. The samples studied were magnetically pure samples, since they have been selected so that the absolute spin number did not exceed the value  $\approx 10^{12}$  spins in each of the sample used before implantation. The temperature of the samples during the implantation was controlled and it did not exceed 400 K.

ESR spectra were registered on X-band ESR-spectrometer "Radiopan" at room temperature by using of  $TE_{102}$  mode rectangular cavity. The ruby standard sample was permanently placed in the cavity on its side-wall. One of the lines of ESR absorption by  $Cr^{3+}$  point paramagnetic centers (PC) was used for the correct relative intensity measurements of ESR absorption, for the calibration of the amplitude value of magnetic component of the microwave field and for precise phase tuning of microwave field. It was possible owing to unsaturating behavior of ESR absorption in ruby in the range of the microwave power applied, which was  $\approx 100$  mW in the absence of attenuation. Unsaturable character of the absorption in a ruby standard was confirmed by means of the measurements of the absorption intensities in two identical ruby samples in dependence on the microwave power level. The first sample was standard sample, permanently placed in the cavity, the second sample was placed in the cavity so that the resonance line intensity was about 0.1 of the intensity of corresponding line of the first sample. They were registered simultaneously but their absorption lines were not overlapped owing to slightly different sample orientations. The foregoing intensity ratio was preserved for all microwave power values in the range used, which indicates, that really ruby samples are good standard samples in ESR spectroscopy studies.

## III. RESULTS

There has been established, that copper and boron HEIBM with implantation direction along  $\langle 111 \rangle$  crystal axis, and boron HEIBM of polycrystalline diamond films with implantation direction transversely to film surface lead to formation of NTs, incorporated in diamond matrix, which possess by relatively weak ferromagnetic ordering. The experimental results were in details represented in [4], [5], [6], [7], and they will be not reproduced

in presented paper. The studies of FMSWR in the sample implanted along  $\langle 110 \rangle$  crystal direction were also described in [7], however we will summarise in the paper presented the experimental results with more details and some new results will be given, which seem to be essential to establish the detailed processes, leading to ferromagnetic ordering formation, since the concrete subsystem, which is responsible for the mechanism of the ferromagnetically ordered state was not proposed in the papers above cited.

The strong anisotropy of FMSWR excitation has been observed in implanted unannealed samples. FMSWR was registered the only in the case, when the implantation plane was perpendicular to the vector  $\vec{H}_1$  of magnetic component of the microwave field. The intensity of FMSWR absorption was increasing with temperature of isochronal 20-minute's annealing up to  $\approx 700$  Celsius degrees. It is interesting, that after the annealing at 350 Celsius degrees and by higher temperatures FMSWR absorption was detected also by the vector  $\vec{H}_1$  of magnetic component of the microwave field position, being to be parallel to sample implantation plane. The parameters of FMSWR absorption, that is splitting parameter, which can be characterised by, for instance, effective g-values of its modes (since central FMSWR-line, which corresponds to ferromagnetic resonance has the only weak anisotropy and it can be considered approximately isotropic if to compare its anisotropy with rather strong anisotropy of FMSWR modes). We will use the g-values of the third mode, Figure 1 for given characteristics. It is seen, that amplitudes, linewidths and intensities of FMSWR modes are also strongly anisotropic, see Figures 2 to 4, where angular dependencies of the linewidth, FMSWR absorption amplitude and intensity of the third FMSWR-mode are presented.

The splitting parameter anisotropy seems to be non-trivial, it characterises by two maxima - at 54.7 degrees, that is, in  $[111]$  direction of diamond lattice, and in direction about 17 degrees from  $[100]$  crystal direction. It is interesting, that the angular dependence of linewidth has the resemblance with the angular dependence of g-value, it characterises also by two maxima at the same angles, see Figure 2. Minimal effective g-value and minimal value of linewidth for the third mode are achieved in the case of  $\langle 110 \rangle$  ion beam modification at  $[110]$  direction. They are equal to 2.1526 and equal to 100 G respectively, maximal effective g-value and maximal value of linewidth correspond to  $[111]$  direction of diamond lattice and are equal respectively to 2.3845 and 360 G. Coincidence of the directions of anisotropy maxima with diamond lattice characteristic directions is indication of the role of host diamond lattice on the characteristics of magnetic ordering, determining the magnetic symmetry, that seems to be possible by relative softness of the corresponding electronic subsystems. Therefore we obtain the strong evidence, that ferromagnetic ordering is determined by electron-electron correlations in valence  $\pi$ -subsystem of electronic system (but not in  $\sigma$ -subsystem), since the

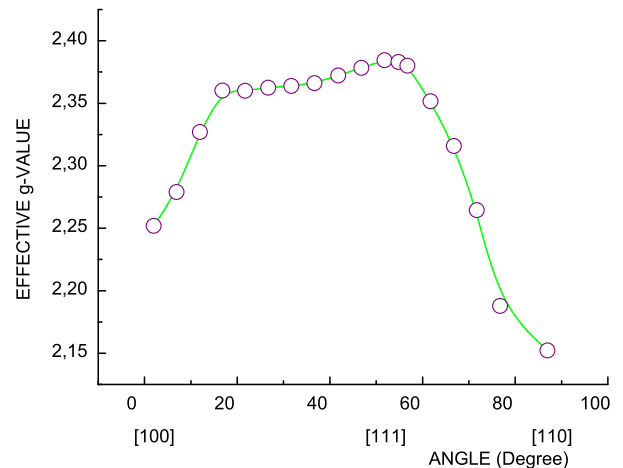


Figure 1: Angular dependence of effective g-value for the third FMSWR-mode, observed in NTs, incorporated in diamond single crystal by nickel ion beam direction transversely  $\langle 110 \rangle$  sample plane

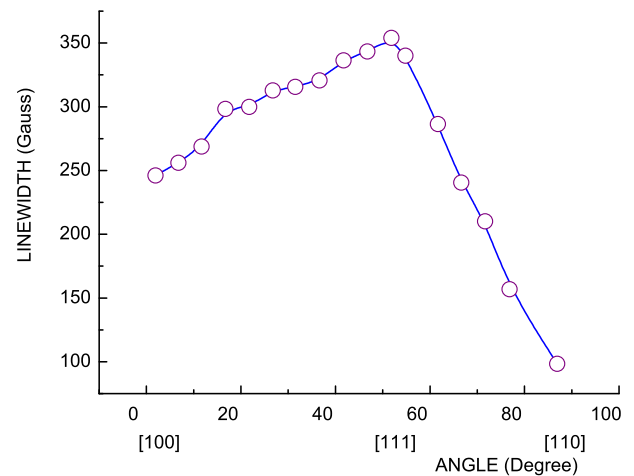


Figure 2: Angular dependence of the linewidth of the third FMSWR-mode, observed in NTs, incorporated in diamond single crystal by nickel ion beam direction transversely  $\langle 110 \rangle$  sample plane

only  $\pi$ -subsystem can be subjected to so strong response (which is mapped by the strong anisotropy of FMSWR-modes above analysed with the axes coinciding with symmetry axes of the host lattice) to the surrounding lattice presence by NT-formation. The  $\sigma$ -subsystem of NTs produced is expected to be not so sensitive to the presence of host diamond lattice. Given prediction is confirmed by formation of own magnetic symmetry with axes, which are not coinciding with symmetry axes of host diamond lattice in NTs, produced by  $\langle 100 \rangle$  ion beam modification.

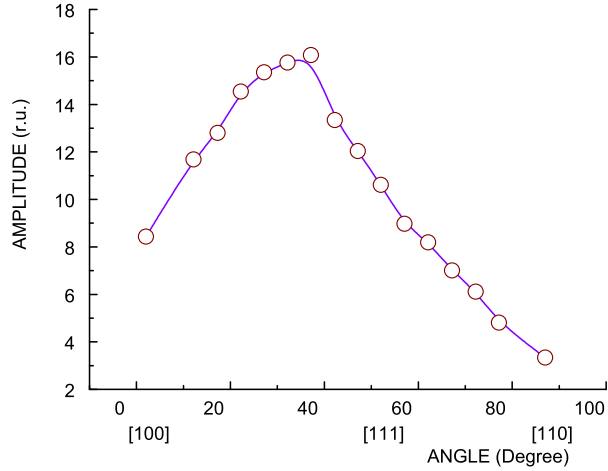


Figure 3: Angular dependence of FMSWR absorption amplitude of the the third FMSWR-mode, observed in NTs, incorporated in diamond single crystal by nickel ion beam direction transversely (110) sample plane

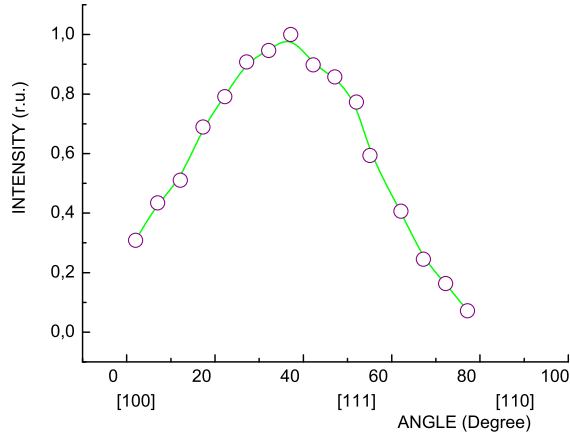


Figure 4: Angular dependence of the FMSWR absorption intensity of the third FMSWR-mode, observed in NTs, incorporated in diamond single crystal by nickel ion beam direction transversely (110) sample plane

It is explained by direct participation of  $\sigma$ -subsystem in magnetic ordering formation, [18].

It is interesting, that, although NT-formation is starting at much more lower ion fluences, the given strong response to diamond lattice presence by initial NT-formation process is preserved by entire HEIBM of near surface region in diamond single crystal. Further, amplitude dependence, Figure 3, is characterised by the clearly pronounced maximum near 35.3 degrees from [100] crystal direction of diamond lattice, that is, it coincides also with symmetry direction of diamond lattice. It is seen,

that amplitude dependence is also strongly anisotropic. Really, the ratio of maximal amplitude value to its minimal value is equal to 4.8. It is additional indication, that mechanism of ferromagnetic ordering is connected with the formation of ordered structures just in  $\pi$ -subsystem of incorporated NTs. Simultaneously, it is the display of the fact, that anisotropy of FMSWR absorption by magnetically ordered NT-structure and the anisotropy of NT-structure itself, which is determined by relatively weak  $g$ -value anisotropy of main resonance mode, are quantitatively different.

Two not very pronounced maxima at 54.7 degrees and in direction near 17 degrees from [100] crystal are appeared additionally to the maximum near 35.3 degrees direction in the angular dependence of the intensity, Figure 4. It is clear, that additional maxima are determined by contribution of linewidth anisotropy, compare Figure 4 and Figure 2.

#### IV. DISCUSSION

Let us indicate once again, that although it was established, that copper and boron HEIBM with implantation direction along  $\langle 111 \rangle$  crystal axis, nickel HEIBM with implantation direction along  $\langle 110 \rangle$  axis, and boron HEIBM of polycrystalline diamond films with implantation direction transversely to film surface lead to formation of NTs, incorporated in diamond matrix, which possess by ferromagnetic ordering, [4], [5], [6], [7], the nature of given state and mechanism, leading to its formation was not strictly theoretically described. To solve given task, it seems to be necessary to know the nature of charge and spin carriers and the mechanisms of carrier transport and interactions of charge and spin carriers both between themselves and with phonons and photons. There seems to be paramount significant the same task for nanoelectronics, spintronics and for the other branches of nanotechnology. There is existing in the theory of 1D electronic systems in particular in the theory of conducting NTs the following concept, which was starting with the work of Tomonaga in 1950, [19], and with the work by Luttinger in 1963, [20], when it has become clear that the electron-electron interaction destroys the sharp Fermi surface and leads to a breakdown of the Landau Fermi liquid (LFL) theory. The resulting non-LFL state is commonly called Luttinger liquid (LL), or sometimes Tomonaga-Luttinger liquid to describe the universal low-energy properties of 1D conductors. LL behavior is characterized by pronounced power-law suppression of the transport current and the density of states, and by effect of spin-charge separation. The nature of the spin and charge carriers was also proposed to be the following. The chargeless spin 1/2 quasiparticles - spinons and spinless quasiparticles with the charge  $\pm e$  - holons were introduced. It was concluded from the universality of LL description that the physical properties do not depend on details of the model, the interaction potential, and

so on, but instead they are only characterized by a few parameters - critical exponents. Further, the LL concept was believed to hold for arbitrary statistical properties of the particles, that is, both for fermions and bosons. It provided a paradigm for non-Fermi liquid physics. When concern the carbon NTs, we have to remark, that there is the following viewpoint. The single-wall carbon nanotubes (SWCNTs) are considered in many works to be 1D objects (it is not always correct, especially for standard NTs with diameter in several nanometers and more) can be described the only in the frame of LL concept. Moreover, SWCNTs are considered even to be the best model system of the LL state demonstration. However, given viewpoint is based the only on experimental observation of power-law behavior by measuring the tunneling conductance of SWNTs in dependence on temperature and voltage and ballistic nature of transport, which was found by electron force microscopic measurements. At the same time spin-charge separation by mechanism of spinons and/or holons' formation has not been observed so far. Therefore, the existing viewpoint seems to be insufficiently grounded, since power-law behavior of the tunneling conductance in dependence on temperature and voltage and ballistic nature of transport phenomena can be explained in the frames of the quite other concepts.

It has to be also remarked, that both the models LL and LFL are the models of ideal (and even oversimplified) quantum liquids, since they do not take into account the nonlinearity of the fermion spectrum on the one hand and electron-phonon interactions on the other hand. In fact both the models describe not strongly adequately the real processes, since the changes in charge state of arbitrary atom in 1D chain to be the result of electron-electron interaction are always accompanied by the changes in phonon subsystem (and vice versa). It is consequence of generic coupling between operators of creation and annihilation in electron subsystem and in phonon field. Let us also remember, that key argument for insertion of the notion "Luttinger liquid" is in fact the simplification, determined by linearization of the generic spectrum of particles in neighborhood of Fermi points in k-space. Just given simplification has led to divergencies arising in the perturbation theory in 1D-case and it does not means that 1D Fermi liquid description is incorrect in general case. Consequently, the description of NTs the only in the frames of LL concept seems to be also oversimplification. Moreover, it is showed in [21], that the concept of description of 1D correlated electronic systems in the frame of 1D Fermi liquid (FL) can be renewed. The most interesting result is that, that the Fermi liquid concept can be applied just to quasi-1D carbon NTs. It was considered in [21] the concept of 1D FL on the example of well known 1D system - *trans*-polyacetylene (t-PL), that is, it is in fact the generalization of well known model developed by Su, Schrieffer, Heeger (SSH-model), [22], [23], [24]. SSH-model, in distinction from LFL and LL models, takes into account the electron-phonon interaction. The subsequent generalization, for instance, for application

of given model immediately to quasi-1D carbon zigzag shaped nanotubes can be easily obtained by using of hypercomplex number theory like to its application in the works, [8], [17], where hypercomplex number theory was used for the interpretation of quantum optics effects in quasi-1D NTs.

Let us summarise briefly for the convenience of the readers the results, presented in [21].

The Born-Oppenheimer approximation was considered and starting Hamiltonian was the following

$$\hat{\mathcal{H}}(u) = \hat{\mathcal{H}}_0(u) + \hat{\mathcal{H}}_{\pi,t}(u) + \hat{\mathcal{H}}_{\pi,u}(u). \quad (1)$$

The first term in (1) is

$$\hat{\mathcal{H}}_0(u) = \sum_m \sum_s \left( \frac{\hat{P}_m^2}{2M^*} \hat{a}_{m,s}^+ \hat{a}_{m,s} + K u_m^2 \hat{a}_{m,s}^+ \hat{a}_{m,s} \right). \quad (2)$$

It represents the sum of operator of kinetic energy of CH-group motion (the first term in (2)) and the operator of the  $\sigma$ -bonding energy (the second term). Coefficient  $K$  in (2) is effective  $\sigma$ -bonds spring constant,  $M^*$  is total mass of CH-group,  $u_m$  is configuration coordinate for  $m$ -th CH-group, which corresponds to translation of  $m$ -th CH-group along the symmetry axis  $z$  of the chain,  $m = \overline{1, N}$ ,  $N$  is number of CH-groups in the chain,  $\hat{P}_m$  is operator of impulse, conjugated to configuration coordinate  $u_m$ ,  $m = \overline{1, N}$ ,  $\hat{a}_{m,s}^+$ ,  $\hat{a}_{m,s}$  are creation and annihilation operators of creation or annihilation of quasiparticle with spin projection  $s$  on the  $m$ -th chain site in  $\sigma$ -subsystem of t-PA.

The second term in (1) can be represented in the form of two components and it is

$$\begin{aligned} \hat{\mathcal{H}}_{\pi,t}(u) &= \hat{\mathcal{H}}_{\pi,t_0}(u) + \hat{\mathcal{H}}_{\pi,t,\alpha_1}(u) = \\ &= \sum_m \sum_s [(t_0(\hat{c}_{m+1,s}^+ \hat{c}_{m,s} + \hat{c}_{m,s}^+ \hat{c}_{m+1,s})) + \\ &+ (-1)^m 2\alpha_1 u] (\hat{c}_{m+1,s}^+ \hat{c}_{m,s} + \hat{c}_{m,s}^+ \hat{c}_{m+1,s}), \end{aligned} \quad (3)$$

where  $\hat{c}_{m,s}^+$ ,  $\hat{c}_{m,s}$  are creation and annihilation operators of creation or annihilation of quasiparticle with spin projection  $s$  on the  $m$ -th chain site in  $\pi$ -subsystem of t-PA. It is the resonance interaction (hopping interaction in tight-binding model approximation) of quasiparticles in  $\pi$ -subsystem of t-PA electronic system, which is considered to be Fermi liquid, and in which the only constant and linear terms in Taylor series expansion of resonance integral about the dimerized state are taking into account.

The expression for the operator  $\hat{\mathcal{H}}_{\pi,u}(u)$ , which describes the part of electron-phonon interaction, determined by interaction between quasiparticles in Fermi liquid state of  $\pi$ -subsystem in terms of  $\{\hat{c}_{k,s}^{(c)}\}$  and  $\{\hat{c}_{k,s}^{(v)}\}$  is the following

$$\hat{\mathcal{H}}_{\pi,u,\alpha_2}(u) = \sum_k \sum_{k'} \sum_s \alpha_2(k, k', s) \hat{c}_{k',s}^{+(c)} \hat{c}_{k',s}^{+(v)} \hat{c}_{k,s}^{(v)} \hat{c}_{k,s}^{(c)}. \quad (4)$$

It has to be indicated, that the operators  $\{\hat{c}_{m,s}^+\}, \{\hat{c}_{m,s}\}$ ,  $m = \overline{1, N}$ , were represented in the form

$$\begin{aligned}\{\hat{c}_{m,s}\} &= \{\hat{c}_{m,s}^{(c)}\} + \{\hat{c}_{m,s}^{(v)}\}, \\ \{\hat{c}_{m,s}^+\} &= \{\hat{c}_{m,s}^{+(c)}\} + \{\hat{c}_{m,s}^{+(v)}\},\end{aligned}\quad (5)$$

related to  $\pi - c$ - and  $\pi - v$ -band correspondingly, and then  $\vec{k}$ -space operators were defined

$$\begin{aligned}\{\hat{c}_{k,s}^{(c)}\} &= \left\{ \frac{i}{\sqrt{N}} \sum_m \sum_s (-1)^{m+1} \exp(-ikma) \hat{c}_{m,s}^{(c)} \right\}, \\ \{\hat{c}_{k,s}^{(v)}\} &= \left\{ \frac{1}{\sqrt{N}} \sum_m \sum_s \exp(-ikma) \hat{c}_{m,s}^{(v)} \right\},\end{aligned}\quad (6)$$

$m = \overline{1, N}$ . The consideration was restricted by the taking into account the contribution of the term, corresponding to interaction between the quasiparticles in different bands, which seems to be the most essential. Physically the identification of linear on displacement  $u$  part of resonance interaction (hopping) and the pairwise interaction of quasiparticles in  $\pi$ -subsystem between themselves with electron-phonon interaction, which was done in cited work, is understandable, if to take into account, that by atomic  $CH$  group displacements the phonons are generated, which in its turn can by release of the place on, for instance,  $(CH)_m$  group, to deliver the energy and impulse, which are necessary for transfer of the quasiparticle (electron) from adjacent  $(m-1)$ - or  $(m+1)$ -position in chain in the case of resonance interaction (hopping). For the case the pairwise interaction of quasiparticles, it means, that its linear on displacement  $u$  part is realized by means of phonon field, which transfers the energy and impulse from one quasiparticle to another (which can be not inevitable adjacent). Mathematically it was proved in the following way. The processes of interaction in  $c$  ( $v$ ) band can be considered to be independent on each other. It means, that transition probability from the  $\langle k_{l,s} |$ -state to  $\langle k_{j,s} |$ -state in  $c$ -band and from  $\langle k'_{l,s} |$ -state to  $\langle k'_{j,s} |$ -state in  $v$ -band, which is proportional to coefficient  $\alpha_2(k, k', s)$ , can be expressed in the form of product of real parts of corresponding matrix elements, that is in the form

$$\begin{aligned}\alpha_2(k, k', s) &\sim Re \langle k_{l,s} | \hat{V}^{(c)} | k_{j,s} \rangle Re \langle k'_{l,s} | \hat{V}^{(v)} | k'_{j,s} \rangle = \\ &\sum_{k_{ph}} Re \langle k_{l,s} | \hat{V}^{(c)} | k_{ph} \rangle \langle k_{ph} | k_{j,s} \rangle \times \\ &\sum_{k_{ph}} Re \langle k'_{r,s} | \hat{V}^{(v)} | k_{ph} \rangle \langle k_{ph} | k'_{n,s} \rangle,\end{aligned}\quad (7)$$

where  $\hat{V}^{(v)} = V_{0(v)} \hat{e}$  ( $\hat{e}$  is unit operator) is the first term in Taylor expansion of pairwise interaction of quasiparticles, for instance, with wave vectors  $k'_r, k'_n$  and spin projection  $s$  in  $v$ -band, that is, in ground state,  $\hat{V}^{(c)} = V_{1(c)} u \hat{e}$  is the second term in Taylor expansion of pairwise interaction in excited state (in  $c$ -band), that is, it is product of configuration coordinate  $u$  and coordinate derivative

at  $u = 0$  of operator of pairwise interaction of quasiparticles with wave vectors  $k_l, k_j$  and spin projection  $s$  in  $c$ -band,  $k_{ph}$  is phonon wave vector, and the summation is realized over all the phonon spectrum. At that, since the linear density of pairwise interaction is independent on  $k$ , which is the consequence of translation invariance of the chain,  $V_{0(v)}, V_{1(c)}$  are constants. Therefore, the pairwise interaction is considered to be accompanying by process of phonon generation, when electronic quasiparticles are already in excited state, that is, in  $c$ -band (retardation effect of phonon subsystem is taken into account). Then it will be  $\hat{V}^{(c)} = V_{0(c)} u \hat{e}$ ,  $\hat{V}^{(v)} = V_{0(v)} \hat{e}$ . A number of variants are possible along with process of phonon generation, corresponding to states of electronic quasiparticles in  $c$ -band above described. The result will mathematically be quite similar, if to change the energetic place of excitation, that is, if to interchange the role of  $c$  and  $v$  bands for given process. There seem to be possible the realization of both the stages (that is phonon generation and absorption) for electronic quasiparticles in single  $c$  or  $v$  band states and simultaneous realisation both the stages in both the bands. Mathematical description will be for all possible variants similar and for distinctness, it was considered only the first variant. For the simplicity, the processes were considered, in which the spin projection is keeping to be the same. Since in  $z$ -direction the impulse distribution is quasi-continuous (the chain has the macroscopic length  $L = Na$ ) the standard way  $\sum_{k_{ph}} \rightarrow \frac{L}{2\pi} \int_{k_{ph}}$  has been used. Further, phonon states were described by wave functions  $\langle k_{ph} | = v_0 \exp(ik_{ph} z)$ , where  $z \in [0, L]$ ,  $k_{ph} \in [-\frac{\pi}{2a}, \frac{\pi}{2a}]$ ,  $v_0$  is constant. Then, it was obtained from (7) the expression

$$\begin{aligned}\alpha_2(k, k', s) &= b |v_{0v}|^2 |v_{0c}|^2 V_{0(c)} u V_{0(v)} |\phi_{0cs}|^2 |\phi_{0vs}|^2 \times \\ &\frac{N}{2\pi(q_l - q_j)(q_r - q_n)} Re \{ \exp[i(k_l m_l - k_j m_j) a] \exp ika \} \times \\ &Re \{ \exp[i(k'_r m_r - k'_n m_n) a] \exp ik'a \},\end{aligned}\quad (8)$$

where  $|\phi_{0cs}|^2, |\phi_{0vs}|^2$  are squares of the modules of the wave functions  $|k_{j,s}\rangle$  and  $|k'_{j,s}\rangle$  respectively,  $k = k_{ph}(q_l - q_j)$ ,  $k' = k'_{ph}(q_r - q_n)$ ,  $q_l, q_j, q_r, q_n \in N$  with additional conditions  $(q_l - q_j)a \leq L$ ,  $(q_r - q_n)a \leq L$ ,  $b$  - is aspect ratio, which in principle can be determined by comparison with experiment. Here the values  $(q_l - q_j)$ ,  $(q_r - q_n)$  determine the steps in pairwise interaction with phonon participation and they are considered to be fixed. The processes, for which  $k = k'$ , were considered. Consequently,  $(q_r - q_n) = (q_l - q_j)$ . Then the Hamiltonian  $\hat{\mathcal{H}}_{\pi,u,\alpha_2}(u)$  was represented in the form

$$\begin{aligned}\hat{\mathcal{H}}_{\pi,u,\alpha_2}(u) &= \\ &\sum_k \sum_{k'} \sum_s 4\alpha_2 u \sin ka \sin k'a a \hat{c}_{k',s}^{+(c)} \hat{c}_{k',s}^{+(v)} \hat{c}_{k,s}^{(v)} \hat{c}_{k,s}^{(c)},\end{aligned}\quad (9)$$

where  $4\alpha_2(s)$  is

$$\frac{b|v_{0v}|^2|v_{0c}|^2V_{0(c)}V_{0(v)}|\phi_{0cs}|^2|\phi_{0vs}|^2 \times N}{2\pi[(q_l - q_j)]^2} = 4\alpha_2(s) \quad (10)$$

Let us remark, that the Hamiltonian  $\hat{\mathcal{H}}_{\pi,u,\alpha_2}(u)$  describes the attraction between the electrons, it can lead to formation of Cooper pairs in a  $\pi$ -subsystem and to superconductivity.

Two values for the energy of quasiparticles, indicating on the possibility of formation of the quasiparticles of two kinds both in  $c$ -band and  $v$ -band have been obtained. They are the following

$$E_k^{(c)}(u) = \frac{Q^2\Delta_k^2 - \epsilon_k^2}{\sqrt{\epsilon_k^2 + Q^2\Delta_k^2}}, \quad (11)$$

$$E_k^{(v)}(u) = \frac{\epsilon_k^2 - Q^2\Delta_k^2}{\sqrt{\epsilon_k^2 + Q^2\Delta_k^2}}$$

and

$$E_k^{(c)}(u) = \sqrt{\epsilon_k^2 + Q^2\Delta_k^2}, \quad (12)$$

$$E_k^{(v)}(u) = -\sqrt{\epsilon_k^2 + Q^2\Delta_k^2}$$

The factor  $Q$  is determined by relation

$$\left[1 + \frac{\alpha_2}{2\alpha_1} \sum_k \sum_s \frac{Q\Delta_k \sin ka}{\sqrt{\epsilon_k^2 + Q^2\Delta_k^2}} (n_{k,s}^{(c)} - n_{k,s}^{(v)})\right] = Q, \quad (13)$$

where  $n_{k,s}^{(c)}$  is eigenvalue of density operator of quasiparticles' number in  $c$ -band,  $n_{k,s}^{(v)}$  is eigenvalue of density operator of quasiparticles' number in  $v$ -band. The quasiparticles with the energy, determined by (12) at  $Q = 1$  are the same quasiparticles, that were obtained in known SSH-model.

Subsequent analysis has showed, that SSH-like solution (12) is inapplicable for the description of standard processes, passing near equilibrium state by any parameters. The quasiparticles, described by SSH-like solution, can be created the only in strongly nonequilibrium state with inverse population of the levels in  $c$ - and  $v$ -bands. At the same time the solution, the energy of quasiparticles for which is determined by (11) can be realised both in near equilibrium and in strongly non-equilibrium states of the  $\pi$ -subsystem of  $t$ -PA, which is considered to be quantum Fermi liquid.

The continuum limit for the ground state energy of the  $t$ -PA chain with SSH-like quasiparticles will coincide with known solution, [23], [24], if to replace  $\Delta_k Q \rightarrow \Delta_k$ . The calculation of the ground state energy  $E_0^{[u]}(u)$  of the  $t$ -PA chain with quasiparticles' branch, which is stable near equilibrium by taking into account, that in ground state  $n_{k,s}^c = 0$ ,  $n_{k,s}^v = 1$ , in the continuum limit gives

$$E_0^{[u]}(u) = -\frac{2Na}{\pi} \int_0^{\frac{\pi}{2a}} \frac{(Q\Delta_k)^2 - \epsilon_k^2}{\sqrt{Q\Delta_k^2 + \epsilon_k^2}} dk + 2NKu^2. \quad (14)$$

Then, calculation of the integral results in the expression

$$E_0^{[u]}(u) = \frac{4Nt_0}{\pi} \left\{ F\left(\frac{\pi}{2}, 1 - z^2\right) + \frac{1 + z^2}{1 - z^2} \left[ E\left(\frac{\pi}{2}, 1 - z^2\right) - F\left(\frac{\pi}{2}, 1 - z^2\right) \right] \right\} + 2NKu^2, \quad (15)$$

where  $z^2 = \frac{2Q\alpha_1 u}{t_0}$ ,  $F(\frac{\pi}{2}, 1 - z^2)$  is the complete elliptic integral of the first kind and  $E(\frac{\pi}{2}, 1 - z^2)$  is the complete elliptic integral of the second kind. Approximation of ground state energy at  $z \ll 1$  for the solution, which is stable near equilibrium position, gives

$$E_0^{[u]}(u) = N \left\{ \frac{4t_0}{\pi} - \frac{6}{\pi} \ln \frac{2t_0}{Q\alpha_1 u} \frac{4(Q\alpha_1)^2 u^2}{t_0} + \frac{28(Q\alpha_1)^2 u^2}{\pi t_0} + \dots \right\} + 2NKu^2. \quad (16)$$

It is seen from (16), that the energy of quasiparticles, described by given solution, has the form of Coleman-Weinberg potential with two minima at the values of dimerization coordinate  $u_0$  and  $-u_0$  like to the energy of quasiparticles, described by SSH-solution. It is understandable, that subsequent considerations, including electrically neutral  $S = 1/2$  soliton and electrically charged spinless soliton formation, that is the appearance of the phenomenon of spin-charge separation, by FL description of 1D systems will be coinciding in its mathematical form with those ones in SSH-model.

It is the main result of the work [21], which means, that the physical properties of 1D systems can be described in the frames of 1D quantum FL including the mechanism of appearance of the most prominent feature of 1D systems - the phenomenon of spin-charge separation.

Since the model proposed takes into consideration the electron-electron correlations in explicit form, it seems to be ground for its application to electronic systems, in which electron-electron correlations are rather strong. In particular, it can be used for analysis of the physical properties including ESR and FMSWR spectra analysis in quasi-1D carbon NTs. It can be done by above indicated manner, that is by using of hypercomplex number theory analogously to theoretical analysis of quantum optics effects in [17] and analysis in [8] of Raman spectra in given objects.

It is substantial, that the mechanism of the phenomenon of spin-charge separation in 1D FL is topological soliton mechanism, which is quite different from Anderson spinon-holon mechanism.

The results obtained show, that the shape of  $\pi$ -solitons (or  $\sigma$ -solitons) is given by the expression having the same mathematical form both in SSH-model and in its FL generalisation. It is

$$|\phi(n)|^2 = \frac{1}{\xi_{\pi(\sigma)}} \text{sech}^2 \left[ \frac{(n - n_0)a}{\xi_{\pi(\sigma)}} - v_{\pi(\sigma)} t \right] \cos^2 \frac{n\pi}{2}, \quad (17)$$

where  $n, n_0$  are variable and fixed numbers of  $CH$ -unit in  $CH$ -chain,  $a$  is  $C - C$  interatomic spacing projection on

chain direction,  $v_{\pi(\sigma)}$  is  $\pi(\sigma)$ -soliton velocity,  $t$  is time,  $\xi_{\pi(\sigma)}$  is  $\pi(\sigma)$  coherence length. It has been shown in [21], that  $\pi$ -solitons ( $\sigma$ -solitons) differ in fact by numerical value of coherence length in SSH-model and in its FL description.

The observation of FMSWR phenomenon in the NTs, formed by  $\langle 110 \rangle$  high energy nickel ion implantation in natural diamond single crystal (at ion beam dose in  $5 \times 10^{14} \text{ cm}^{-2}$ ) unambiguously means, that the SSH  $\pi$ -soliton lattice formation takes place, that is periodical non-harmonic spin-density wave. For the simplicity we can approximate the function of the shape of given density wave (let us designate it with abbreviation ASLSDW and ASLCDW (Approximation of Soliton Lattice Spin (Charge) Density Wave) by trapeziform function, Fig-

ure 5. Real function of the envelope shape of soliton lattice spin density wave will be between given trapeziform function and harmonic sinusoidal function for density wave (HSDW - Harmonic Spin Density Wave). We will show, that given approximation is rather good for qualitative and in the principle for quantitative estimation of characteristics of ferromagnetic order formation in carbon NTs. The calculation in [9] will be adapted for given case. Actually, from mathematical viewpoint the difference between ASLSDW and HSDW states is minimal, since ASLSDW can be represented in the form of superposition of HSDWs, where amplitude of main harmonic is strongly exceeding the others. It follows from the expansion of ASLSDW profile in Fourier series, which is

$$f(x') = A(2L_0 + L_1) \sum_{m=0}^{\infty} \left\{ \frac{[2(2L_0 + L_1) \left( \cos \frac{\pi m L_0}{2L_0 + L_1} - \cos \frac{\pi m (L_0 + L_1)}{2L_0 + L_1} \right) - \pi L_1 m \sin m\pi]}{2L_1 \pi^2 m^2} \cdot \cos \frac{2\pi m x'}{L} \right\}, \quad (18)$$

$$f(x) = A(2L_0 + L_1) \left[ \frac{1}{4} + (2L_0 + L_1) \sum_{m=1}^{\infty} \frac{\left( \cos \frac{\pi m L_0}{2L_0 + L_1} - \cos \frac{\pi m (L_0 + L_1)}{2L_0 + L_1} \right)}{2L_1 \pi^2 m^2} \cdot \cos \frac{2\pi m x}{L} \right]. \quad (19)$$

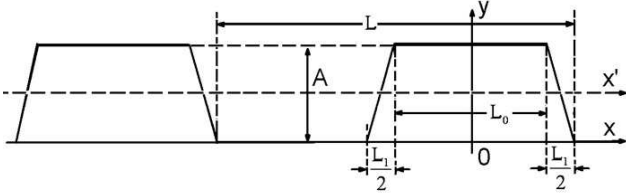


Figure 5: Approximation of soliton lattice spin (charge) density wave profile along the chain direction

The sense of the parameters  $L_0$ ,  $L_1$ ,  $L$  is seen from Figure 5. The functions  $f(x)$ ,  $f(x')$  denote spin density distributions  $S(x)$ ,  $S(x')$  in the case of ASLSDW and charge density distributions  $\rho(x)$ ,  $\rho(x')$  in the case of ASLCDW. Expression (18) corresponds to position of chain atoms along  $X'$ -direction, Figure 5. Expression (19) corresponds to position of chain atoms along  $X$ -direction, Figure 5. We see, that by asymmetric deviation of spin (or charge) density relatively the chain direction, the constant component is appeared. It will lead in the case of soliton lattice formation to ferromagnetic ordering if density wave distribution is magnetic spin density wave distribution and to ferroelectric ordering by similar electric dipole density distribution. It is clear from (18) and (19), that the amplitude of components with  $m > 1$  is inversely proportional to  $m^2$ , that

is, it diminishes rather quickly when number  $m$  increases. In the first order approximation, the relations (18) and (19) can be represented by

$$f(x') = A(2L_0 + L_1) \alpha \cos \frac{2\pi x'}{L} + o\left(\frac{1}{m^2}\right), \quad (20)$$

$$f(x) = A(2L_0 + L_1) \left( \frac{1}{4} + \frac{1}{2} \alpha \cos \frac{2\pi x}{L} \right) + o\left(\frac{1}{m^2}\right), \quad (21)$$

where  $\alpha$  is

$$\alpha = \frac{[2(2L_0 + L_1) \left( \cos \frac{\pi L_0}{2L_0 + L_1} - \cos \frac{\pi (L_0 + L_1)}{2L_0 + L_1} \right)]}{L_1 \pi^2}. \quad (22)$$

It is seen from (17), that envelope function of single soliton spin density distribution corresponds precisely to the case with  $x$  axis position, that is, it is strongly asymmetric relatively the chain axis. By the formation of the soliton lattice the periodic envelope function of soliton spin density distribution in soliton lattice will be determined by overlapping of individual envelope functions and the asymmetry extent can be even more pronounced depending on overlapping extent.

Let us also remark, that given conclusion is preserved, when simultaneously with Peierls metal-insulator transition the Mott-Hubbard metal-insulator transition also takes place. It leads to modification of oscillating factor



in (17). Instead of factor  $\cos^2 \frac{n\pi}{2}$  the factor  $(b_1 \cos^2 \frac{n\pi}{2} - b_2 \sin^2 \frac{n\pi}{2})$  is appeared, at that in real case of t-PA the value of  $b_1$  is substantially exceeds  $b_2$ , although  $b_2$  is nonzero, [25].

The viewpoint above developed agrees well with results of the work [26], where the real lineshapes of SSH-soliton line in t-PA, registered by both ESR and electron-nuclear double resonance (ENDOR), were approximated even with rectangular spin-density distribution (that is, by particular case of trapeziform distribution at  $L_1 = 0$ ). It seems to be essential, that real ESR lineshape was fitted by given distribution very well by  $\xi_\pi = 24a$  and  $b_2/b_1 = 0.3$  and qualitatively the lineshape of ENDOR spectrum, which is substantially more sensitive to choose of shape function, was also reproduced at the same parameters  $\xi_\pi = 24a$  and  $b_2/b_1 = 0.3$ .

Further, it was found also, that there is numerical coincidence of the characteristics of SSH topological  $\pi$ -solitons in t-PA and in quasi-1D CZSNTs, formed both by  $\langle 111 \rangle$  and  $\langle 110 \rangle$  ion implantation. So, the values of  $g$ -tensor components in  $Cu$ -implanted sample are  $g_1 = 2.00255$  (it is minimal  $g$ -value and it is  $g_{||}$  principal direction),  $g_2 = g_3 = g_\perp = 2.00273$ , the accuracy of relative  $g$ -value measurements is  $\pm 0.00002$ , [4]. It is substantial, that  $g$ -value of paramagnetic  $\pi$ -solitons in t-PA, equaled to 2.00263, [27], gets in the middle of given rather narrow interval of  $g$ -value variation of PC in ion produced NTs. Although anisotropy of paramagnetic  $\pi$ -solitons in t-PA, mapping the distribution of  $\pi$ -electron density along the whole individual t-PA chain, was not resolved by ESR measurements in [27] directly, there are indirect evidences on axial symmetry of ESR absorption spectra in t-PA too, [26], [28]. Consequently, the value 2.00263 is average value and it coincides with accuracy 0.00002 with average value of aforecited principal  $g$ -tensor values of PC in quasi-1D CZSNTs. Taking into account given high precision coincidence of  $g$ -values in t-PA and quasi-1D CZSNTs we can conclude that SSH-soliton density distribution in quasi-1D CZSNTs is also asymmetric along hypercomplex  $x$ -axis.

Therefore, the appearance of ferromagnetic ordering in quasi-1D CZSNTs, formed by  $\langle 111 \rangle$  and  $\langle 110 \rangle$  ion im-

plantation, for which the only  $\pi$ -subsystem is responsible is experimentally confirmed.

Thus we have found the physical origin of the mechanism of the formation of ferromagnetic ordering in carbon NTs. It is determined the only by  $\pi$ -subsystem of full electronic system, which agrees well with experimental results on FMSWR above summarised and explains qualitatively the sensitivity of the symmetry of FMSWR parameters, Figures 1 to 4, to symmetry directions of surrounding diamond crystal lattice in NTs, produced by  $\langle 110 \rangle$  implantation by relative softness of  $\pi$ -subsystem in comparison with  $\sigma$ -subsystem. Given conclusion agrees well with the results of the work [18], where the participation of  $\sigma$ -subsystem in magnetic ordering formation in NTs, produced by  $\langle 100 \rangle$  implantation, leads to own magnetic symmetry, the main symmetry axes for which are not coinciding with symmetry axes of the host diamond lattice.

## V. CONCLUSIONS

The physical origin of the mechanism of the formation of ferromagnetic ordering in carbon nanotubes produced by high energy ion beam modification of diamond single crystals in  $\langle 110 \rangle$  and  $\langle 111 \rangle$  directions has been established. It is determined by asymmetry of spin density distribution of Su-Schrieffer-Heeger topological soliton lattice, which is formed in 1D Fermi quantum liquid state of the only  $\pi$ -electronic subsystem of given NTs. The conclusions are based on detailed analysis of angular dependencies of the parameters of ferromagnetic spin wave resonance, numerical values and symmetry of  $g$ -values of main FMSWR moxdes, taking into account the theory of 1D Fermi liquid and adaptation of the calculation, which gives the qualitative evaluation of total magnetization and indicates on the appearance of ferromagnetic ordering by the formation of  $\pi$ -electronic SSH-soliton lattice (produced by spin 1/2 SSH solitons in 1D Fermi  $\pi$ -electronic liquid) with asymmetric spin distribution relatively 1D hypercomplex symmetry axis of NTs studied.

- 
- [1] Erchak D.P, Penina N.M, Stelmakh V.F, Tolstykh VP, Zaitsev AM, The 7th Int.Conf.IBMM 90, Abstracts, Knoxville, USA, 1990, p.313
  - [2] Efimov V.G, Erchak D.P, Gelfand R.B, Penina N.M, Stelmakh V.F, VS Varichenko, Ulyashin A.G, Zaitsev AM, E-MRS 1990 Fall Meeting, Abstracts, Strasbourg, France, 1990, p.C-V/P 12
  - [3] Kawataba K., Mizutani M., Fukuda M., Mizogami S., Synthetic Metals, **33** (1989) 399-402
  - [4] Erchak D.P, Efimov V.G, Zaitsev AM, Stelmakh V.F, Penina N.M, Varichenko VS, Tolstykh VP, Nuclear Instrum.Meth.in Phys.Res.,B, **69** (1992) 443-451
  - [5] Erchak D.P, Guseva M.B, Alexandrov A.F, Alexander H, Pilar v.Pilchau A, Pis'ma v Zhurnal Experimentalnoi i Teoreticheskoi Fiziki, **58**, N 4 (1993) 268-271, JETP Letters, **58**, N 4 (1993) 275-278
  - [6] Ertchak D.P, Efimov V.G, Stelmakh V.F, Review, Zhurnal Prikladnoi Spektroskopii, **64**, N 4 (1997) 421-449, J.Applied Spectroscopy, **64**, N 4, (1997) 433-460
  - [7] Ertchak D.P, Efimov V.G, Stelmakh V.F, Martinovich V.A, Alexandrov A.F, Guseva M.B, Penina N.M, Karpovich I.A, Varichenko V.S, Zaitsev A M, Fahrner W.R, Fink D, Physica Status Solidi, b, **203**, N2 (1997) 529-548
  - [8] Yerchuck D, Dovlatova A, J.Phys.Chem.,C, DOI: 10.1021/jp205549b, **116**, N 1 (2012) 63-80
  - [9] Yearchuck D, Yerchak Y, Alexandrov A, Phys.Lett.A,

- 373**, N 4 (2009) 489-495
- [10] Hulthen L, Proc.Roy.Acad.Sci.(Amsterdam), **39** (1936) 190
  - [11] Anderson P W, Phys.Rev., **86** (1952) 694
  - [12] Keffer F, Thesis, Berkeley, January 1952
  - [13] Keffer F, Kaplan H, Yafet Y, American Journal of Physics, **21**, N 4 (1953) 250-257
  - [14] Ziman J M, Proc.Phys.Soc.(London), **A65** (1952) 540
  - [15] Nakamura T., Progr.Theor.Phys., **7** (1952) 539
  - [16] Tani K., Progr.Theor.Phys., **31**, N 3 (1964) 335-356
  - [17] Dovlatova A, Yearchuck D, Chem.Phys.Lett., **511** (2011) 151-155
  - [18] Yerchuck D, Stelmakh V, Dovlatova A, Yerchak Y, Alexandrov A, in press
  - [19] Tomonaga S., Prog.Theor.Phys., **5** (1950) 544
  - [20] Luttinger J M, J.Math.Phys., **4** (1963) 1154
  - [21] A.Dovlatova, D.Yerchuck, F.Borovik, in press
  - [22] Su W.P., Schrieffer J.R, and Heeger A.J, Phys.Rev.Lett., **42** (1979) 1698
  - [23] Su W.P., Schrieffer J.R, and Heeger A.J, Phys.Rev.B, **22**, (1980) 2099
  - [24] Heeger A.J, Kivelson S, Schrieffer J.R, Su W-P, Rev.Mod.Phys., **60** (1988) 781-850
  - [25] Thomann H, Dalton L R, Grabowsky M, Clarke T C, Phys.Rev.B, **31** (1985) 3141
  - [26] Kahol P K, Mehring M, J.Phys.C, **19** (1986) 1045-1054
  - [27] Goldberg, I B; Crowe, H R; Newman, P R; Heeger, A.J; MacDiarmid, A G, J.Chem.Phys., **70** (1979) 1132-1135
  - [28] Kuroda S., Tokumoto M., Kinoshita N., Shirakawa H., J.Phys.Soc.Jpn., **51** (1982) 693-694

# Room Temperature Superconductivity and Uncompensated Antiferromagnetic Ordering in Carbon Nanotubes

Dmitri Yerchuck (a), Vyacheslav Stelmakh (b), Alla Dovlatova (c), Yauhen Yerchak (b), Andrey Alexandrov (c)  
(a) - Heat-Mass Transfer Institute of National Academy of Sciences of RB, Brovka Str.15, Minsk, 220072, dpy@tut.by  
(b) - Belarusian State University, Nezavisimosti Avenue 4, Minsk, 220030, RB  
(c) - M.V.Lomonosov Moscow State University, Moscow, 119899  
(Dated: November 17, 2018)

The phenomenon of formation of uncompensated antiferromagnetic ordering coexisting with superconductivity at room temperature in carbon nanotubes, produced by high energy ion beam modification of diamond single crystals in (100) direction is argued.

PACS numbers: 71.10.-w, 73.63.Fg, 78.30.-j, 76.30.-v, 76.50.+g, 78.67.-n  
Keywords:

## I. INTRODUCTION AND BACKGROUND

Discovery of new types of superconducting materials has accelerated in 21st century. The commencement of 21th century was commemorated by the discovery of superconductivity, which was observed at relatively high temperature  $T_c = 40$  K in the simple (structurally and electronically) compound  $MgB_2$  [1]. The origin of its is understood to be arising from charge carriers, which turn out to be placed into very strongly bonding states. They in its turn respond very sensitively to the bond-stretching vibrational modes, see, for instance [2], [3], [4]. The boron-boron bonds in the graphite-like layers of  $MgB_2$  are rather strong, and it is argument to the appearance of superconductive state. At the same time, the graphite itself and diamond are materials that have even stronger bonds (in graphene plane in the case of graphite).

Consequently, it allows to consider the carbon and carbon-based materials to be perspective materials for the realization of superconducting states.

Really, the second step in the field was the discovery of superconductivity at 4 K in very heavily boron-doped diamond, reported in 2004 by Ekimov et al [5]. Confirmation has been provided by Takano et al, who reported the value of transition temperature to superconducting state  $T_c$  equaled to 7 K in B-doped diamond films [6].

The origin of of superconductivity in diamond was discussed in a number of theoretical works, see for example [7], [8]. In [7], an ab initio study of the superconductivity of boron doped diamond within the framework of a phonon-mediated pairing mechanism was presented. It has been shown in [7], that the role of the dopant, in substitutional position, is unconventional in that half of the coupling parameter  $\alpha$  originates in strongly localized defect-related vibrational modes, yielding a very peaked Eliashberg function (spectral decomposition of  $\alpha$ ). The electron-phonon coupling potential was found to be extremely large, however  $T_c$  remained to be low because of the low value of the density of states at the Fermi level (hat is connected with 3D nature of the network). The authors of [7] have invited to study the case

of doped diamond surfaces, where both the contraction of the reconstructed bonds and the 2D nature of the surface states may lead to much larger  $T_c$ . We will show, that given idea, concerning of 2D nature of the carbon states by preservation of bond strength (that allows to generate high frequency phonons) is actually true. The same idea (however in implicit form) is presented in [8], where the superconductivity of boron-doped diamond is studied in comparison with its analogy with  $MgB_2$ . So, it was found, that the deformation potential of the hole states arising from the C-C bond stretch mode in diamond is 60 percents larger than the corresponding quantity in  $MgB_2$  that drives its high  $T_c$ . It leads to very large electron-phonon matrix elements. The evaluated coupling strength coefficient  $\alpha$  by using in [8] of rather simplified approach leads nevertheless to  $T_c$  values in the only 5-10 K range, in agreement with experiment (although in [8] the rather simplified approach has been used). Hence, it makes phonon coupling to be the likely mechanism. Really, let us to represent the key points for given conclusion.

(1) The carrier states are the very strongly covalent bonding states, that makes diamond so hard.

(2) The carrier states should be sensitively coupled to the bond-stretching mode, which lies at the very high frequency of  $1332\text{ cm}^{-1}$  (0.16 eV) in diamond.

Both ingredients are the same ones prevailing in  $MgB_2$ . There are differences, both of a positive and negative nature. In  $MgB_2$ , the only two of the nine phonon branches are bond-stretching, whereas in diamond three of the six phonon branches are bond-stretching. On the other hand,  $MgB_2$  is strongly two dimensional in its significant  $\sigma$ -bands, which means a near-step-function increase in the density of participating states by doping, the states in diamond are three-dimensional and their Fermi level density of states  $N(0)$  increases with doping level essentially more slowly.

Authors of [8] conclude, that higher doping should increase  $T_c$  somewhat, but effects of three dimensionality primarily on the density of states will keep doped diamond from having a  $T_c$  closer to that of  $MgB_2$ .

Therefore, authors of above cited works come indepen-

dently to the same conclusions concerning the nature of superconductivity in heavily boron-doped diamond. It has to be remarked, that discovery of superconductivity in diamond followed the discovery of superconductivity in doped silicon clathrates [9] ( $T_c = 8$  K), a cage-like silicon material which crystallizes in the same  $sp^3$  environment. Let us also remark, that even though the reported temperatures are rather low by  $sp^3$  environment, the superconducting transition of column IV semiconductors is of much interest, since it concerns very common materials, in which column IVa elements in Mendeleev Periodic Table are based elements.

The aforesaid idea to use 2D-modification of column IVa elements was successfully realized relatively recently (in 2008) in the work [10] and the essential progress in  $T_c$  enhancement up to 145 K was achieved. In [10] the transition to the superconducting state in the silicon sandwich S-Si-QW-S nanostructures prepared by short time diffusion of boron after preliminary oxidation of the n-type Si (100)-surface has been found. The sandwich S-Si-QW-S structures represent themselves the p-type high mobility silicon quantum wells (QW) confined by the nanostructured  $\delta$ -barriers heavily doped with boron on the n-type Si (100)-surface. The studies of the cyclotron resonance angular dependences, the scanning tunneling microscopy images and the electron spin resonance (ESR) have shown, that the nanostructured  $\delta$ -barriers consist of a series of alternating undoped and doped quantum dots, with the doped dots containing the single trigonal ( $C_{3v}$ -symmetry) dipole centers,  $B_+ + B_-$ , which are produced by the negative-U reconstruction of the shallow boron acceptors,  $2B_0 \rightarrow B_+ + B_-$ . The temperature and magnetic field dependencies of the resistance, thermo-emf (Seebeck coefficient), specific heat and magnetic susceptibility were studied and gave clear evidence of the high temperature superconductivity,  $T_c = 145$  K. It, according to [10], seems to be resulting from the transfer of the small hole bipolarons through the  $B_+ + B_-$  dipole centers at the Si-QW- $\delta$ -barrier interfaces. The value of the superconductor energy gap has been found to be equal 0.044 eV. The extremely low value of the hole effective mass in the sandwich S-Si-QW-S structures that has been derived from the measurements of the Shubnikov - de Haas oscillations is considered by authors to be the principal argument for the bipolaronic mechanism of high temperature superconductor properties that is based on the coherent tunneling of bipolarons.

The next success of the first decade of 21th century in the field of superconductivity studies was the discovery of superconductivity coexisting with antiferromagnetic ordering in the iron-based layered pnictide compound LaFeAsO (that is, also in material with prevailed 2D-dimensional structure). It was reported approximately in the same time with the discovery of Bagraev et al (in 2008) in [11]. Next, the superconductivity has been discovered in both oxygen containing RFeAsO (R = La, Nd, Sm) compounds and in oxygen free  $AFe_2As_2$  (A = Ba, Sr, Ca) compounds. It is interesting, that the su-

perconductivity occurs upon doping into the FeAs layers of either electrons or holes. Let us remark, that owing to the highly two-dimensional structure the pnictides are like to the cuprates. It gave rise to the viewpoint that the physics of the pnictides is similar to the cuprates, and involves insulating behavior. However, there is a growing consensus among researchers that Mott-transition physics does not play a significant role for the iron pnictides, and there are strong indications, that magnetic order is of spin-density wave (SDW) type rather than Heisenberg antiferromagnetism of localized spins. In particular, it is evidenced by a relatively small value of the observed magnetic moment per Fe atom, which is around 12–16 percents of  $2\mu_B$ . In another distinction to the cuprates, electronic structure, which was proposed by band-structure calculations and was supported by angle-resolved photoemission spectroscopy, consists of two small hole pockets centered around  $\Gamma$  point,  $\vec{k} = (0, 0)$  and of two small electron pockets centered around M point  $\vec{k} = \vec{Q} = (\pi, \pi)$  in the folded Brillouin zone (BZ) (two Fe atoms in the unit cell).

Many theoretical studies are devoted at present to the study of superconductivity state (SSt) formation in pnictides. For instance, the authors of the paper [12] have presented Fermi-liquid analysis of SDW magnetism and superconductivity in given compounds. They considered a two-band model with small hole and electron pockets located near  $\Gamma$  and M points in the folded BZ and argued, that for the geometry indicated, particle-hole and particle-particle channels are nearly identical, and the interactions logarithmically increase at low energies. It has been found, that the interactions in the SDW and extended s-wave ( $s^+$  - wave) channels  $\vec{k} = (0, 0)$ ,  $\vec{k} = \vec{k} + \vec{Q}$  become comparable in strength being to be the result of the increase in the intraband pair hopping term and the reduction in the Hubbard-type intraband repulsive interaction. The authors also argued, that at zero doping, SDW instability comes first, but at a finite doping,  $s^+$  ( $s^\pm$  in designation by other authors) superconducting instability occurs at a higher temperature.

The  $s^+$  pairing bears similarity to magnetically mediated  $d_{x^2-y^2}$  pairing in systems with large Fermi surface (FS) with an idea that in both cases the pairing comes from repulsive interaction, peaked at  $\vec{Q}$ , and requires the gap to change its sign under  $\vec{k} \rightarrow \vec{k} + \vec{Q}$ . The difference is that for small pockets, the gap changes sign away from the Fermi surface and remains constant along the FS. Spin response of a clean and doped  $s^+$  superconductor is analysed in [12] and it has been found that

- (i) it possesses a resonance mode which disperses like to Anderson-Bogolyubov mode, that is, with the same velocity,
- (ii) intraband scattering by nonmagnetic impurities does not affects the system, but interband scattering affects the system in the same way like to magnetic impurities in an s-wave superconducting state.

Let us touch now on the nature of magnetic ordering

in carbon and carbon based materials too. It is well known, that all substances on the whole are magnetics and that classical magnetic ordering is existing in the substances, which are built from the atoms with unfilled inner atomic  $d$ - or  $f$ -shells or include given atoms in their elementary units. In other words, magnetically ordered solid substances are the groups of substances, elementary units of which include transition chemical elements with unfilled atomic 3d-, 4d-, 5d-, 6d-shells, or 4f, 5f-shells of rare earth elements. Carbon does not refer to given groups. At the same time, there are at present a number of reports on magnetic ordering in carbon and carbon based materials.

On the experimental revealing of magnetic ordering in carbon structurally ordered systems was reported for the first time during the IBMM-Conference in Knoxville, TN, USA [13] and it was confirmed in report on E-MRS Conference in Strasbourg, France [14]. Let us remark, that the first report almost in the same time on magnetic ordering in structurally non-ordered carbon materials is the work [15], where ferromagnetic ordering in pyrolytic carbon, produced by chemical vapour deposition method was found. Let us also remark, that simultaneously, the reports [13], [14] were the first reports on the formation by high energy ion beam modification (HEIBM) of diamond single crystals structurally and magnetically ordered quasi-one-dimensional (quasi-1D) system along ion tracks, that is, on the formation of new carbon allotropic form, which was identified with nanotubes (NTs), incorporated in diamond matrix. It was shown, that axes of incorporated NTs are very precisely coinciding with ion beam direction [16]. Given NTs were found to be produced also in polycrystalline diamond films with implantation direction transversely to film surface [17]. They possess by a number of interesting physical properties, reported in [16], [17], [19], [18]. When concern the magnetic ordering, it was established from the study of temperature dependence of electron spin resonance absorption intensity, that, for instance, incorporated nanotubes, produced by neon HEIBM of diamond single crystal along  $\langle 100 \rangle$  crystallographic direction, possess by weak antiferromagnetic ordering [16], [19], [18]. At the same time, copper HEIBM with implantation direction along  $\langle 111 \rangle$  crystal axis, nickel HEIBM with implantation direction along  $\langle 110 \rangle$  axis [16], [19], [18] and boron HEIBM of polycrystalline diamond films with implantation direction transversely to film surface [17] lead to formation of NTs, incorporated in diamond matrix, which possess by ferromagnetic ordering. It was established directly by observation of ferromagnetic spin wave resonance (FM-SWR) [17], [19], [18]. It was found, that magnetic ordering is inherent property for given carbon electronic system and it is not connected with magnetic impurities, since starting samples were selected in that way, that the absolute spin number of paramagnetic impurities and the other paramagnetic structural imperfections in the samples studied did not exceed the value  $\sim 10^{12}$  spins. Very recently [20], antiferroelectric ordering has been

found in the same pure carbon allotropic form - quasi-1D carbon zigzag-shaped nanotubes (CZSNTs), obtained by boron- and copper-HEIBM of diamond single crystals in  $\langle 111 \rangle$ -direction. It was established by means of the detection of new optical phenomenon - antiferroelectric spin wave resonance (AFESWR), which was theoretically described and experimentally confirmed for the first time by infrared (IR) spectroscopy studies of carbynes and polyvinylidenhalogenides in [21]. Let us indicate on some significant conclusions, which were done on base of foregoing results. Given results mean, that pure carbon in the form of quasi-1D CZSNTs and carbyne chains are multiferroic systems. In its turn, the experimental observation of multiferroicity in quasi-1D CZSNTs and carbynes means the breakdown of space inversion symmetry along CZSNT hypercomplex (that is, along  $n$ -dimensional symmetry axis  $z$ , see [22], [20], where  $n$  is the number on the chain in CZSNT) and along carbyne chain symmetry axis. In the case of CZSNTs, it agrees well with the model of quasi-1D CZSNTs [22], [20], based on bond dimerization in all chain components of quasi-1D CZSNT along its hypercomplex symmetry axis  $z$ , which actually leads to inversion symmetry breakdown along given axis. It is evident, that inversion symmetry breakdown gives necessary condition for the appearance of nonzero polarisation by atomic displacements, that is for antiferroelectricity (however it seems to be not sufficient condition in general case).

Qualitatively, the appearance of magnetic ordering in carbon systems can be understandable, if to take into account, that free carbon atoms have spin value  $S = 1$  and orbital moment value  $L = 1$  with opposite direction, resulting in compensation of each other. It is clear, that in condensed carbon compounds given situation can be changed by both the change of orbital moment direction and/or its value. It means, that on carbon base (and on the base of the other IV-group elements - Si, Ge, free atoms of which have also spin value  $S = 1$  and orbital moment value  $L = 1$  with opposite direction) can be produced the materials with magnetic properties to be comparable with those ones, which possess the substances, elementary units of which include transition chemical elements with unfilled atomic 3d-, 4d-, 5d-, 6d-shells, or 4f-, 5f-shells of rare earth elements. The mechanisms to achieve given goal can be very different. One of the mechanisms was discussed in [23].

The aim of given work is to study in more details the properties of non-cylindrical nanotubes, produced in diamond single crystals by high energy ion implantation, which are possessing instead of  $C_\infty$  symmetry axis the only by  $C_4$  symmetry axis and to establish the mechanisms of formation of magnetic and electric ordering in given NTs. They seems to be the appropriate candidates for high temperature superconducting systems, since both the mechanisms of superconductivity like to those ones established in  $MgB_2$  and in pnictides, briefly reviewed above, can be realized (see Section IV). Moreover, it will be theoretically shown, that usual s-wave

mechanism, proposed by Bardeen, Cooper, Schrieffer (BCS) [24] can also be realized. In other words, multicannel superconductivity is predicted in given NTs.

Let us remark, that non-cylindrical nanotubes, incorporated in diamond single crystals, are representing the quite new class of carbon structures, since they cannot be considered to be limit case of fullerene series (whereas it takes place for cylindrical nanotubes). It is the consequence of the alternating-sign curvature of the four-petal NT-surface in the direction, being to be transversal to NT-axis (the curvature of cylindrical nanotubes like to fullerenes is not alternating-sign).

## II. EXPERIMENTAL TECHNIQUE

Samples of type IIa natural diamond, implanted by high energy ions of nickel (the energy of ions in ion beam was 335 MeV) have been studied. Paramagnetically pure samples have been selected so that the absolute spin number did not exceed the value  $\approx 10^{12}$  spins in each of the samples used before implantation. Ion implantation was performed along  $\langle 100 \rangle$  crystal direction (ion beam dose was  $5 \times 10^{13} \text{ cm}^{-2}$ ) transversely to sample (100)-plane uniformly along all the plane surface. The temperature of the samples during the implantation was controlled and it did not exceed 400 K. ESR spectra were registered on X-band ESR-spectrometer "Radiopan" at room temperature by using of  $TE_{102}$  mode rectangular cavity. The ruby standard sample was permanently placed in the cavity on its sidewall. One of the lines of ESR absorption by  $Cr^{3+}$  point paramagnetic centers (PC) in ruby was used for the correct relative intensity measurements of ESR absorption, for the calibration of the amplitude value of magnetic component of the microwave field and for precise phase tuning of modulation field. The correct relative intensity measurements become to be possible owing to unsaturating behavior of ESR absorption in ruby in the range of the microwave power applied, which was  $\approx 100 \text{ mW}$  in the absence of attenuation. Unsaturable character of the absorption in a ruby standard was confirmed by means of the measurements of the absorption intensities in two identical ruby samples in dependence on the microwave power level. The first sample was standard sample, permanently placed in the cavity, the second sample was placed in the cavity away from the loop of magnetic component of microwave field so, that its resonance line intensity was about 0.1 of the intensity of corresponding line of the first sample. Both the samples were registered simultaneously but their absorption lines were not overlapped owing to slightly different sample orientations. The foregoing intensity ratio was precisely preserved for all microwave power values in the range used, which indicates, that really ruby samples are good standard samples in ESR spectroscopy studies.

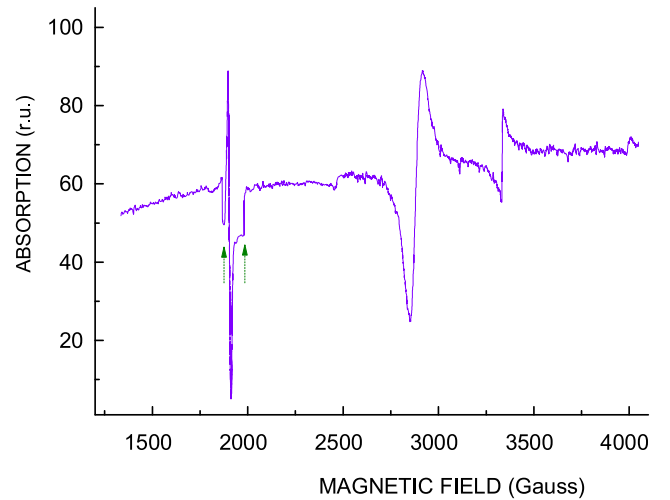


Figure 1: Spectral distribution of ESR absorption intensity in diamond single crystal, implanted by high energy nickel ions by beam direction transversely (100) sample plane, the sample was rotated in  $(0\bar{1}1)$  plane,  $\vec{H}_0 \parallel [100]$  crystal axis, leftmost line belongs to ruby standard

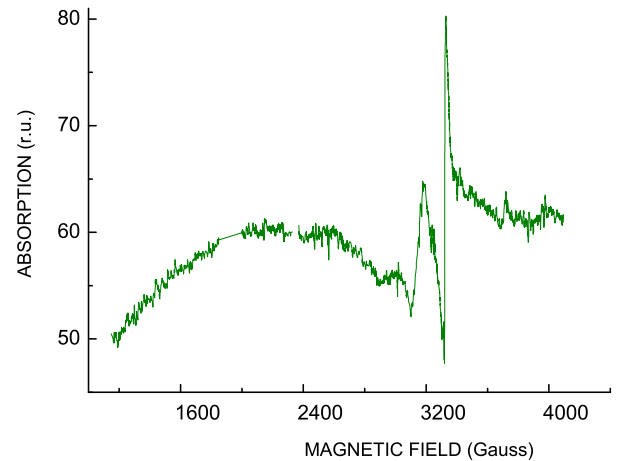


Figure 2: Spectral distribution of ESR absorption intensity in diamond single crystal, implanted by high energy nickel ions by beam direction transversely (100) sample plane, the sample was rotated in  $(0\bar{1}1)$  plane,  $\vec{H}_0 \parallel [111]$  crystal axis

## III. RESULTS

The ESR spectra observed in carbon nanotubes, produced by nickel high energy  $\langle 100 \rangle$  ion beam modification of natural diamond single crystals, are presented in Figures 1 to 3 in crystal directions  $[100]$ ,  $[111]$  and 60 degrees from  $[100]$  correspondingly. The line in the range (1865 - 1981) G (given field range is indicated by arrows in Figure 1) is the absorption line by ruby standard, it is shifted to bottom in Figure 1 and it is removed in the same range in

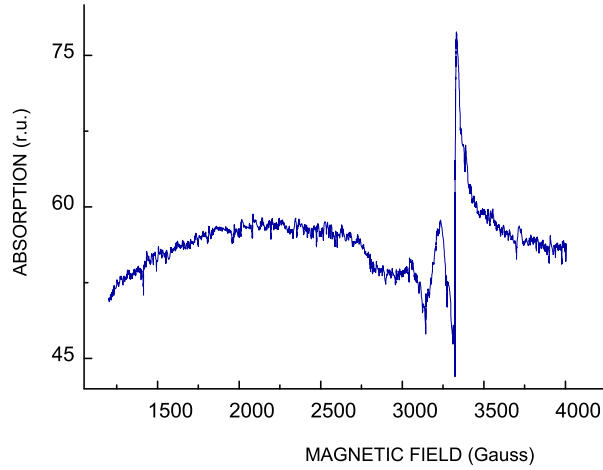


Figure 3: Spectral distribution of ESR absorption intensity in diamond single crystal, implanted by high energy nickel ions by beam direction transversely (100) sample plane, the sample was rotated in (011) plane, the angle between  $\vec{H}_0$  and [100] crystal axis is 60 degrees

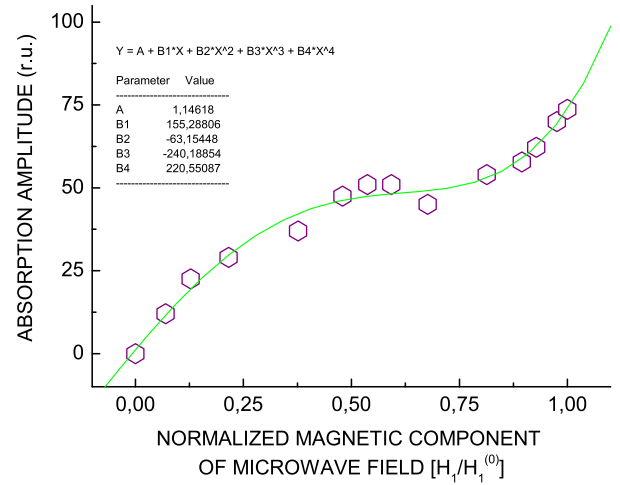


Figure 5: Dependence of absorption amplitude of the right broad line  $R_b$  in ESR spectrum of NTs incorporated in diamond single crystal on magnetic component of microwave field at  $\vec{H}_0 \parallel [100]$  crystal axis

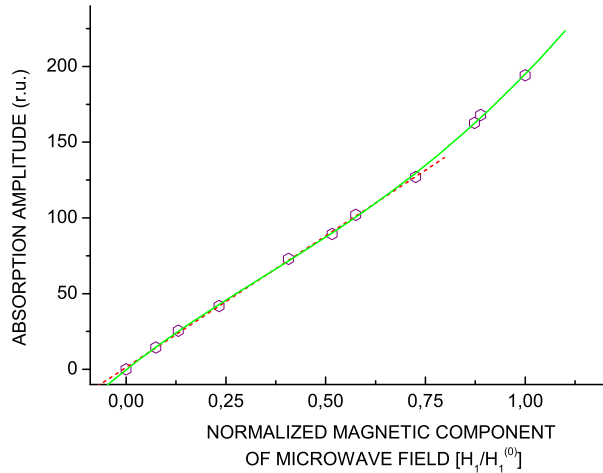


Figure 4: Dependence of absorption amplitude of the left line L in ESR spectrum of NTs incorporated in diamond single crystal on magnetic component of microwave field at  $\vec{H}_0 \parallel [100]$  crystal axis

Figure 2. The most intensive two lines, belonging to the sample studied, were excited spontaneously the only by very precise orientation of external static magnetic field  $\vec{H}_0$  in the plane coinciding with the plane, transversal to implantation plane and containing the implantation direction. Therefore, resulting spectrum was consisting of three lines, at that two new lines have rather large anisotropic linewidths. Let us designate given lines by  $R_b$  for the right broad line and by L for the left line.

The right broad line was overlapped with relatively narrow almost isotropic line, designated by  $R_n$  (given line was observed by usual sample orientation). Additionally, very broad strongly intensive anisotropic absorption was observed. It consists of two backgrounds with two dip positions (in integrated spectrum) at  $\sim 2410$  G and  $\sim 2892$  G by spectrum registration in the direction corresponding to [111] diamond lattice direction, Figure 2. Dip positions for given background absorption were coinciding by static magnetic field direction in 60 degrees from [100] diamond crystal direction, Figure 3. It seems to be the display of the fact, that the symmetry of the interaction, leading to the appearance of very strong background absorption is determined by inherent symmetry of NTs, produced by [100] HEIBM, which is not connected with potential effect of diamond lattice presence.

Dependencies of absorption amplitudes of L-line and  $R_b$  line on magnetic component of microwave field at fixed orientation of polarising magnetic field  $\vec{H}_0 \parallel [100]$  crystal axis have been studied, Figures 4 and 5. It is seen from comparison of the Figures 4 and 5, that given dependencies are quite different. The dependence, presented for L-line in Figure 4, is superlinear. It is similar to the dependencies, which were earlier observed in the samples, modified by HEIBM with copper, neon, nickel ions (however with dose  $5 \times 10^{14}$ ) [16], [19], [18], that is, in the case of entire modification of diamond layer, which is localised near implantation surface. It means, that the layer was consisting then the only of NTs, which seem to be interacting each other. In the studied sample (integral dose is  $5 \times 10^{13}$ ), individual NTs are isolated by diamond structure, nevertheless the superlinear dependence is taking place, which seems to be unexpected. Let

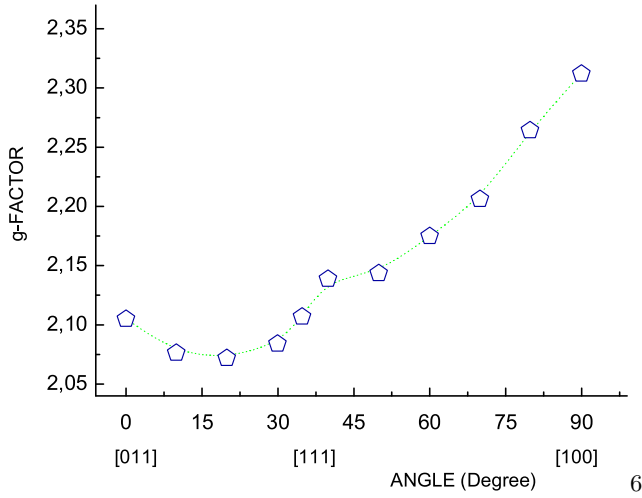


Figure 6: Angular dependence of g-factor of the left line L in ESR spectrum of NTs incorporated in diamond single crystal, the sample was rotated in  $(0\bar{1}1)$  plane

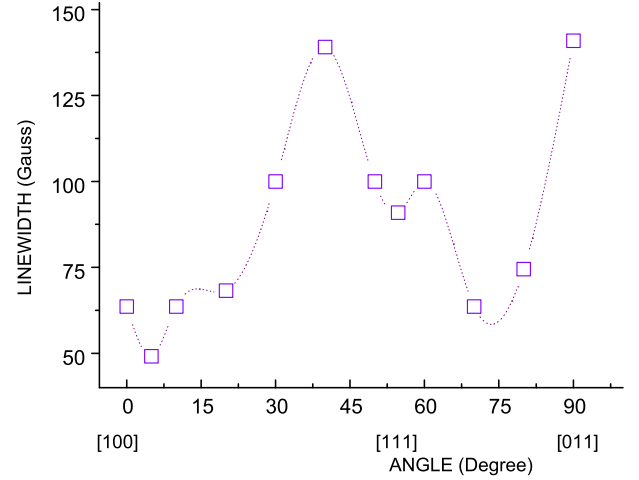


Figure 8: Angular dependence of linewidth of the left line L in ESR spectrum of NTs incorporated in diamond single crystal, the sample was rotated in  $(0\bar{1}1)$  plane

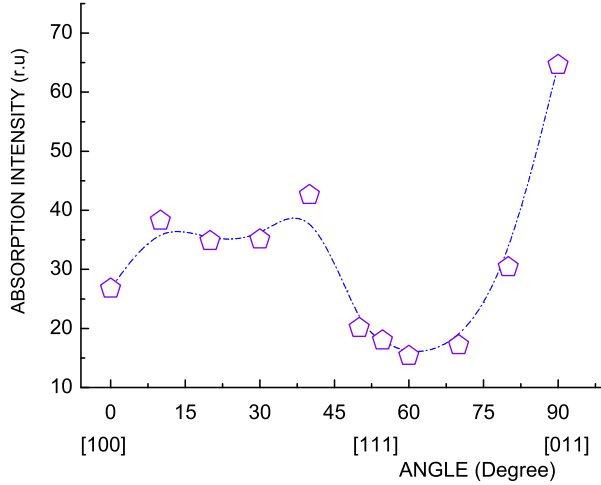


Figure 7: Angular dependence of ESR absorption intensity of the left line L in ESR spectrum of NTs incorporated in diamond single crystal, the sample was rotated in  $(0\bar{1}1)$  plane

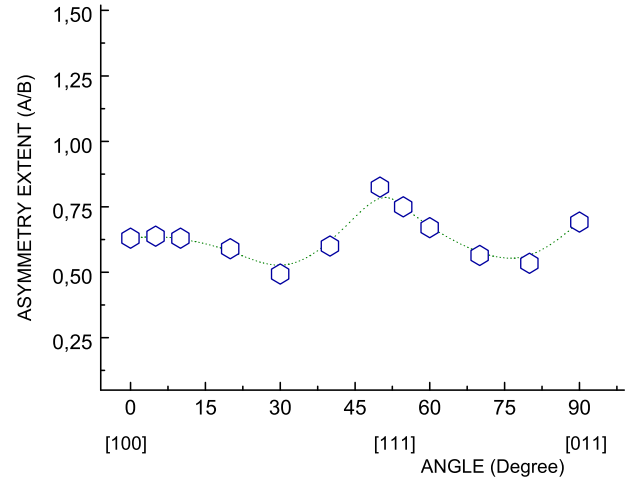


Figure 9: Angular dependence of asymmetry extent A/B of the left line L in ESR spectrum of NTs incorporated in diamond single crystal, the sample was rotated in  $(0\bar{1}1)$  plane

us remark, that the initial part of the curve, presented in Figure 4, can in the principle be approximated by a linear dependence (dashed line), although it is clear from comparison with the approximation of the whole curve, solid line in Figure 4, that even initial part, strongly speaking, is not linear. Solid line in Figure 4 is the polynomial fit with the function  $f(x) = b_0 + b_1x + b_2x^2 + b_3x^3 + b_4x^4$ , where  $b_0 = -0.17117$ ,  $b_1 = 208.92305$ ,  $b_2 = -139.06624$ ,  $b_3 = 159.14424$ ,  $b_4 = -33.90983$ .

Dependence of absorption amplitude of the right broad line  $R_b$  in ESR spectrum of NTs on magnetic component of microwave field is strongly nonlinear. It is characterised for the values of relative magnetic component of

microwave field  $H_1/H_1^{(0)}$  in the range (0-0.75) by usual saturating law, but in the range (0.75-1) it acquires prominent superlinear nonsaturating character. The dependence for ESR absorption kinetics in the form, presented in Figure 5, is observed in ESR-spectroscopy for the first time. It can be approximated by the solid line, which represents itself the polynomial fit in accordance with relation  $Y(x) = A + B_1x + B_2x^2 + B_3x^3 + B_4x^4$ , where  $A = 1.14618$ ,  $B_1 = 0.77956$ ,  $B_2 = -0.00159$ ,  $B_3 = -3.03868e^{-5}$ ,  $B_4 = 1.40072e^{-7}$ . Angular dependence of g-factor of the left line L in ESR spectrum of



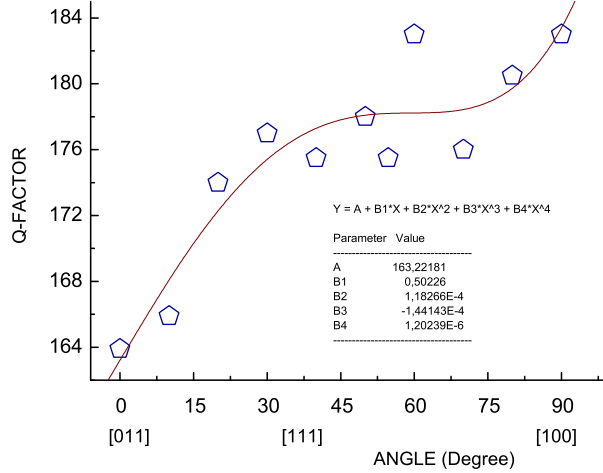


Figure 10: Angular dependence of the cavity Q-factor with the sample implanted by high energy nickel ions by beam direction transversely (100) sample plane, the sample was rotated in (011) plane

NTs in the sample studied is presented in Figure 6. It consist of two branches. One branch is in the angle range 0-50 degrees from [100] crystal lattice direction (which is coinciding with NT axis direction), the second branch is in the angle range 50-90 degrees. Let us remark, that the connection point of two branches, equaled to 50 degrees for the g-values of L-line is not coinciding with the point of the junction of two dips in the very broad (and consequently very intensive) absorption, testifying on the existence of two different resonance processes, which are responsible for the appearance of L-line and very broad lines. The deviation of g-values from free electron value  $g = 2.0023$  is very large, at that the minimal value is achieved in the range 16-20 degrees from the [011] direction in diamond lattice and it is equal to  $\approx 2.0719$ , maximal g-value corresponds to NT axis direction, that is to [100] crystal lattice direction and it is equal to  $\approx 2.3120$ . Given values are characteristic for the systems with the strong magnetic ordering. Consequently, we have obtained the direct proof of the spontaneous transition of NT system, incorporated in diamond lattice, in the state with the strong magnetic ordering. Angular dependence of ESR absorption intensity of the left line L has qualitatively opposite character to g-factor dependence. The maximal absorption value corresponds to the direction, being to be transversal to NT axis, which is coincides with [011] direction in diamond lattice, Figure 7. Additional maximum is observed at 60 degrees from given direction. Let us remark, that both the maxima in angular dependence of ESR absorption intensity of the line L are observed also in angular dependence of linewidth, Figure 8, indicating, that the main features in angular dependence of ESR absorption intensity are governed by angular dependence of linewidth. It is confirmed also by

that, the very pronounced maximum in the angular dependence of absorption amplitude of line L is in the range 10-20 degrees from [100] crystal lattice direction (the corresponding Figure is not presented). At the same time it is not pronounced in angular dependence of absorption intensity, see Figure 7. It is seen from angular dependence of linewidth of the line L, Figure 8, that its value is strongly dependent on direction of the static magnetic field applied. There are four maxima, main maximum is achieved at [011] direction with linewidth value, which is equal to 140.9 G, very pronounced maximum is observed at the angle in 40 degrees from [100] lattice direction, linewidth value is equal to 139.1 G, that is, it is comparable with main maximum value. Two, not very pronounced maxima are observed correspondingly at the angle between 10 and 20 degrees and at the angle in 60 degrees from [100] lattice direction, linewidth values are equal correspondingly to 68.7 G and 100 G. Main minimum is achieved near NT axes' direction, more strictly at  $\approx 5$  degrees from given direction with linewidth value, which is equal to 49.1 G. The foregoing linewidth values are characteristic for the states with strong magnetic ordering, that is, it is additional argument in favour of the conclusion on the formation of strong magnetic ordering in the sample studied. It is also seen from Figure 8, that two branches of linewidth growth, starting at  $\approx 5$  degrees and in the range 70-75 degrees from [100] direction, have the resemblance. That seems to be the indication on the same origin of linewidth broadening process, determining foregoing growth branches.

Especially interesting, that the line L is asymmetric, Figure 9. However, the angular dependence of the ratio  $A/B$  of the asymmetry extent is disagreeing with the angular dependence, which has to be observed by usual Dyson effect in metals or semiconductors [25]. The value  $B/A$  is equal 2.55 for static (immobile) paramagnetic centers (PC) in conductive media in the case of thick samples and it is determined by the space dispersion contribution [26], which is appeared in conductive media. It corresponds to the ratio of space dispersion contribution and absorption contribution to resulting ESR response equal to (1 : 1) [26]. The value  $B/A$  for absorption derivative is increasing from 2.55 to more than 19 for mobile PC (or by presence of spin diffusion) in dependence on the velocity of mobile PC (or on the rate of the spin diffusion) [27]. In the case of thin samples, the ratio  $B/A$  has intermediate values, between 1 and above indicated, depending on the thickness of the samples. It is seen from Figure 9, that the ratio  $A/B$  is anisotropic. The maximal  $A/B$  value (correspondingly, minimal  $B/A$ ) is near [111] crystal lattice direction and it is equal to 0.83, Figure 9. The minimal  $A/B$  (maximal  $B/A$ ) value is near 60 degrees from [011] crystal lattice direction and it is equal to 0.49, Figure 9. Let us remark, that by usual Dyson effect in conducting thin samples (in particular in the samples with metallic NTs, producing the network) the maximal deviation from the ratio  $A/B = 1$  has to be observed by microwave field propagation direction along the sample

side with maximal size of implanted region in rotation plane, that is by  $H_0$  along [100] crystal direction, in the case, when the network is opaque for microwave field in direction, transverse to NT axis direction, or by  $H_0$  along [011] in the case, when the network is opaque the only for microwave field propagation in direction, coinciding with NT axes. The observed maximal deviation of ratio  $A/B$  from  $A/B = 1$  at  $\approx 60$  degrees from [011] confirms the conclusion on nontrivial nature of Dyson-like effect in the sample studied.

The presence of the ruby standard allowed to control the cavity  $Q$ -factor, Figure 10. It seems to be substantial, that  $Q$ -factor is increasing in the ranges, where deviation of ratio  $A/B$  from  $A/B = 1$  is also increasing, that is, increase is starting near 60 degrees from [011] crystal lattice direction and increase takes place in the range near 10-30 degrees from the same [011] crystal direction, compare Figures 10 and 9. For usual Dyson effect it has to be conversely,  $Q$ -factor has to be minimal in the direction of maximal deviation of ratio  $A/B$  from  $A/B = 1$ , that is near 30 degrees from [100] crystal lattice direction, Figure 9. It is seen from Figure 10, that  $Q$ -factor has in given direction the maximal value, which indicates simultaneously, that the approximation by solid line has to be more accurate (more of experimental points is required).

#### IV. DISCUSSION

It will be further argued, that the results above described are agreed with spontaneous transition of the system to the state which characterises by coexistence simultaneously of antiferromagnetic (AFM) uncompensated ordering and superconductivity, which is realized in electron spin resonance conditions and it is absent without resonance. Given specific conditions seem to be indicating, that the nature of given state and mechanisms, leading to its formation cannot be entirely coinciding with known ones, including above reviewed. To solve given task, it seems to be necessary to know the nature of charge and spin carriers and the mechanisms of carrier transport and interactions of charge and spin carriers both between themselves and with phonons and photons in NTs studied. There seems to be paramount significant the same task for nanoelectronics, spintronics and for the other branches of nanotechnology. Let us remark, that in the theory of 1D electronic systems, in particular, in the theory of conducting NTs is existing the following concept. It is based on the work of Tomonaga [28] and on the work of Luttinger [29], from which follows, that the electron-electron interaction destroys the sharp Fermi surface and leads to a breakdown of the Landau Fermi liquid (LFL) theory for 1D systems. The resulting non-LFL state is commonly called Luttinger liquid (LL), or sometimes Tomonaga-Luttinger liquid (TLL). Given approach was used upto now for description of the universal low-energy properties of all 1D conductors.

The theory of LL (TLL) predicts the pronounced power-law suppression of the transport current and the density of states, and the effect of spin-charge separation. The nature of the spin and charge carriers according to LL (TLL) theory is the following. They are chargeless spin  $1/2$  quasiparticles - spinons and spinless quasiparticles with the charge  $\pm e$  - holons. The universality of LL (TLL) description means that the physical properties of 1D systems have to be not depending on details of the model, of the interaction potential, and so on. They are only characterized by a few parameters - critical exponents. Quite remarkably, that the LL (TLL) concept is believed to be valid for arbitrary statistical properties of the particles, that is both for fermions and bosons. It is interesting that along with a paradigm for non-Fermi liquid physics for description of any 1D systems the concept of LL (TLL) was extended for description of 2D and 3D correlated electrons in systems with linear dispersion law.

Concerning NTs, let us remark, that the single-wall carbon nanotubes (SWCNTs) are considered in many works to be 1D objects (it is not always correct, especially for standard NTs with diameter in several nanometers and more), which can be described the only in the frame of LL (TLL) concept. Moreover, SWCNTs are considered to be the best model systems for the LL state demonstration. The arguments used to confirm given conclusion are the following. It is the experimental observation of power-law behavior by measuring the tunneling conductance of SWNTs in dependence on temperature and voltage. It has to be remarked however, that power laws are widely spread in the physics. They can approximate some other dependences or can follow from the other theories too. Electron force microscopic measurements showed also the ballistic nature of transport in conducting SWNTs, predicted by the LL (TLL) model. Ballistic behavior of transport phenomena can also be determined by the other causes, not connected with LL (TLL) model. Insufficiency of the substantiation of the applicability of LL (TLL) model to SWCNTs becomes to be evident, if to take into account, that main feature, of given model - spin-charge separation by spinon-holon mechanism has not been observed.

It has to be also taken into account, that both the models LL (TLL) and LFL are the models of ideal quantum liquids. Moreover, both the models are oversimplified, since they do not take into account the nonlinearity of the fermion spectrum on the one hand and the presence of electron-phonon interactions on the other hand. In fact both the models describe not strongly adequately the real processes, since the changes in the charge state of arbitrary atom in 1D chain, being to be the result of electron-electron interaction, are always accompanied by the changes in phonon subsystem (and vice versa). It is consequence of generic coupling between operators of creation and annihilation in electron subsystem and in phonon field (see further for more details). Let us also remember, that key argument for insertion of the no-

tion "Luttinger liquid" itself is in fact also based on the simplification, determined by linearization of the generic spectrum of particles in neighborhood of Fermi points in  $k$ -space. At the same time the divergencies arising in the perturbation theory in 1D-case are the consequence just of given simplification. From here it is not follows, that 1D Fermi liquid description is incorrect in general case, which takes into account the electron-phonon interaction and/or nonlinearity of the generic spectrum of particles in neighborhood of Fermi points in  $k$ -space.

So we come to conclusion, that the description of NTs the only in the frames of LL concept seems to be also oversimplification. Moreover, it is showed in [30] that the concept of description of 1D correlated electronic systems wihtin the framework of 1D Fermi liquid (FL) can be restored.

It was considered in [30] the concept of 1D FL on the example of well known 1D system - *trans*-polyacetylene (t-PL). It is in fact the generalization of well known model of organic 1D conductors proposed by Su, Schrieffer, Heeger (SSH-model) [31], [32], which is formally Fermi gas model. It will be futher shown that SSH-model takes the intermediate position between Fermi gas and Fermi liquid models, since it takes into consideration the electron-electron correlations in implicit form. The further generalization, for instance, for application of 1D FL model immediately to quasi-1D carbon zigzag shaped nanotubes can be obtained by using of hypercomplex number theory like to the works [22], [20], where hypercomplex number theory was applied for the interpretation of quantum optics effects in carbon zigzag shaped NTs.

Let us represent for the convenience of the readers the main moments of calculation and the results of the work [30].

The Born-Oppenheimer approximation was considered and starting Hamiltonian was the following

$$\hat{H}(u) = \hat{H}_0(u) + \hat{H}_{\pi,t}(u) + \hat{H}_{\pi,u}(u). \quad (1)$$

The first term in (1) is

$$\hat{H}_0(u) = \sum_m \sum_s \left( \frac{\hat{P}_m^2}{2M^*} \hat{a}_{m,s}^+ \hat{a}_{m,s} + K u_m^2 \hat{a}_{m,s}^+ \hat{a}_{m,s} \right). \quad (2)$$

It represents itself the sum of operator of kinetic energy of CH-group motion (the first term in (2)) and the operator of the  $\sigma$ -bonding energy (the second term). Coefficient  $K$  in (2) is effective  $\sigma$ -bonds spring constant,  $M^*$  is total mass of CH-group,  $u_m$  is configuration coordinate for  $m$ -th CH-group, which corresponds to translation of  $m$ -th CH-group along the symmetry axis  $z$  of the chain,  $m = \overline{1, N}$ ,  $N$  is number of CH-groups in the chain,  $\hat{P}_m$  is operator of impulse, conjugated to configuration coordinate  $u_m$ ,  $m = \overline{1, N}$ ,  $\hat{a}_{m,s}^+$ ,  $\hat{a}_{m,s}$  are creation and annihilation operators of creation or annihilation of quasiparticle with spin projection  $s$  on the  $m$ -th chain site in  $\sigma$ -subsystem of t-PA. The second term in (1) can be represented in the form of two components and it is

$$\begin{aligned} \hat{H}_{\pi,t}(u) &= \hat{H}_{\pi,t_0}(u) + \hat{H}_{\pi,t,\alpha_1}(u) = \\ &= \sum_m \sum_s [(t_0(\hat{c}_{m+1,s}^+ \hat{c}_{m,s} + \hat{c}_{m,s}^+ \hat{c}_{m+1,s})) + \\ &+ (-1)^m 2\alpha_1 u] (\hat{c}_{m+1,s}^+ \hat{c}_{m,s} + \hat{c}_{m,s}^+ \hat{c}_{m+1,s}), \end{aligned} \quad (3)$$

where  $\hat{c}_{m,s}^+$ ,  $\hat{c}_{m,s}$  are creation and annihilation operators of creation or annihilation of quasiparticle with spin projection  $s$  on the  $m$ -th chain site in  $\pi$ -subsystem of t-PA. It is the resonance interaction (hopping interaction in tight-binding model approximation) of quasiparticles in  $\pi$ -subsystem of t-PA electronic system, which is considered to be Fermi liquid, and in which the only constant and linear terms in Taylor series expansion of resonance integral about the dimerized state are taking into account.

Operator  $\hat{H}(u)$  is invariant under spatial translations with period  $2a$ , where  $a$  is projection of spacing between two adjacent CH-groups in undimerized lattice on chain axis direction, and which is equal to  $1.22 \text{ \AA}$ . It means, that all various wave vectors  $\vec{k}$  in  $\vec{k}$ -space will be in reduced zone with module of  $\vec{k}$  in the range  $-\frac{\pi}{2a} \leq k \leq \frac{\pi}{2a}$  [32]. Reduced zone is considered like to usual semiconductors to be consisting of two subzones - conduction ( $c$ ) band and valence ( $v$ ) band. Then the operators  $\{\hat{c}_{m,s}^+\}$ ,  $\{\hat{c}_{m,s}\}$ ,  $m = \overline{1, N}$ , were represented in [30] in the form

$$\begin{aligned} \{\hat{c}_{m,s}\} &= \{\hat{c}_{m,s}^{(c)}\} + \{\hat{c}_{m,s}^{(v)}\}, \\ \{\hat{c}_{m,s}^+\} &= \{\hat{c}_{m,s}^{+(c)}\} + \{\hat{c}_{m,s}^{+(v)}\}, \end{aligned} \quad (4)$$

related to  $\pi - c$ - and  $\pi - v$ -band correspondingly, and  $\vec{k}$ -space operators were defined

$$\begin{aligned} \{\hat{c}_{k,s}^{(c)}\} &= \left\{ \frac{i}{\sqrt{N}} \sum_m \sum_s (-1)^{m+1} \exp(-ikma) \hat{c}_{m,s}^{(c)} \right\}, \\ \{\hat{c}_{k,s}^{(v)}\} &= \left\{ \frac{1}{\sqrt{N}} \sum_m \sum_s \exp(-ikma) \hat{c}_{m,s}^{(v)} \right\}, \end{aligned} \quad (5)$$

$m = \overline{1, N}$ .

The  $\sigma$ -operators  $\{\hat{a}_{m,s}^+\}$  and  $\{\hat{a}_{m,s}\}$ ,  $m = \overline{1, N}$  were also represented in the form like to (4) for  $\pi$ -operators and analogous to (5), transforms was defined. It leads to the following expression for the operator  $\hat{H}_0(u)$

$$\hat{H}_0(u) = \sum_k \sum_s \left( \frac{\hat{P}_k^2}{2M^*} + K u^2 \right) (\hat{n}_{k,s}^{\sigma,c} + \hat{n}_{k,s}^{\sigma,v}), \quad (6)$$

where  $\hat{n}_{k,s}^{\sigma,c}$  and  $\hat{n}_{k,s}^{\sigma,v}$  are operators of number of  $\sigma$ -quasiparticles in  $\sigma$ - $c$ -band and  $\sigma$ - $v$ -band correspondingly.

The independence of  $|u_m|$  on  $m$ ,  $m = \overline{1, N}$ , was taken into consideration.

The expression for  $\hat{H}_{\pi,t_0}(u)$  in terms of  $\{\hat{c}_{k,s}^{(c)}\}$  and  $\{\hat{c}_{k,s}^{(v)}\}$  is coinciding with known corresponding expression in [31], [32] and it is

$$\hat{H}_{\pi,t_0}(u) = \sum_k \sum_s 2t_0 \cos ka (\hat{c}_{k,s}^{+(c)} \hat{c}_{k,s}^{(c)} - \hat{c}_{k,s}^{+(v)} \hat{c}_{k,s}^{(v)}) \quad (7)$$

The expression for the second part of operator  $\hat{\mathcal{H}}_{\pi,t}(u)$  in terms of  $\{\hat{c}_{k,s}^{(c)}\}$  and  $\{\hat{c}_{k,s}^{(v)}\}$  is also coinciding in its form with known corresponding expression in [31], [32] and it is given by

$$\hat{\mathcal{H}}_{\pi,t,\alpha_1}(u) = \sum_k \sum_s 4\alpha_1 u \sin ka (\hat{c}_{k,s}^{+(v)} \hat{c}_{k,s}^{(c)} + \hat{c}_{k,s}^{+(c)} \hat{c}_{k,s}^{(v)}), \quad (8)$$

where subscript  $\alpha_1$  in Hamiltonian designation indicates on the taking into account the part of electron-phonon interaction, connected with resonance interaction (hopping) processes. The expression for the operator  $\hat{\mathcal{H}}_{\pi,u}(u)$ , which describes the part of electron-phonon interaction, determined by interaction between quasiparticles in Fermi liquid state of  $\pi$ -subsystem in terms of  $\{\hat{c}_{k,s}^{(c)}\}$  and  $\{\hat{c}_{k,s}^{(v)}\}$  is the following

$$\hat{\mathcal{H}}_{\pi,u,\alpha_2}(u) = \sum_k \sum_{k'} \sum_s \alpha_2(k, k', s) \hat{c}_{k',s}^{+(c)} \hat{c}_{k',s}^{+(v)} \hat{c}_{k,s}^{(v)} \hat{c}_{k,s}^{(c)}. \quad (9)$$

The contribution of the term, corresponding the only to interaction between the quasiparticles in different bands, which seems to be the most essential, was considered. The expression for  $\alpha_2(k, k', s)$  was obtained in the form

$$\alpha_2(k, k', s) = b |v_{0v}|^2 |v_{0c}|^2 V_{0(c)} u V_{0(v)} |\phi_{0cs}|^2 |\phi_{0vs}|^2 \times \frac{N}{2\pi(q_l - q_j)(q_r - q_n)} \text{Re}\{\exp[i(k_l m_l - k_j m_j)a] \exp ika\} \times \text{Re}\{\exp[i(k'_r m_r - k'_n m_n)a] \exp ik'a\}, \quad (10)$$

where  $|\phi_{0cs}|^2$ ,  $|\phi_{0vs}|^2$  are squares of the modules of the wave functions  $|k_{j,s}\rangle$  and  $|k'_{j,s}\rangle$  respectively,  $k = k_{ph}(q_l - q_j)$ ,  $k' = k'_{ph}(q_r - q_n)$ ,  $q_l, q_j, q_r, q_n \in N$  with additional conditions  $(q_l - q_j)a \leq L$ ,  $(q_r - q_n)a \leq L$ ,  $b$  - is aspect ratio, which in principle can be determined by comparison with experiment. Here the values  $(q_l - q_j)$ ,  $(q_r - q_n)$  determine the steps in pairwise interaction with phonon participation and they are considered to be fixed. The processes, for which  $k = k'$ , are considered. Consequently,  $(q_r - q_n) = (q_l - q_j)$  and the operator  $\hat{\mathcal{H}}_{\pi,u,\alpha_2}(u)$  is

$$\hat{\mathcal{H}}_{\pi,u,\alpha_2}(u) = \sum_k \sum_{k'} \sum_s 4\alpha_2(s) u \sin ka \sin k'a \hat{c}_{k',s}^{+(c)} \hat{c}_{k',s}^{+(v)} \hat{c}_{k,s}^{(v)} \hat{c}_{k,s}^{(c)}, \quad (11)$$

where  $\alpha_2(s)$  is

$$\alpha_2(s) = \frac{b}{4} |v_{0v}|^2 |v_{0c}|^2 V_{0(c)} V_{0(v)} |\phi_{0cs}|^2 |\phi_{0vs}|^2 \times \frac{N}{2\pi[(q_l - q_j)]^2} \quad (12)$$

The system of operators  $\hat{c}_{k',s}^{+(c)}$ ,  $\hat{c}_{k',s}^{+(v)}$ ,  $\hat{c}_{k,s}^{(v)}$ ,  $\hat{c}_{k,s}^{(c)}$  corresponds to noninteracting quasiparticles, and it is understandable, that in the case of interacting quasiparticles

their linear combination has to be used

$$\begin{bmatrix} \hat{a}_{k,s}^{(v)} \\ \hat{a}_{k,s}^{(c)} \end{bmatrix} = \begin{bmatrix} \alpha_{k,s} & -\beta_{k,s} \\ \beta_{k,s} & \alpha_{k,s} \end{bmatrix} \begin{bmatrix} \hat{c}_{k,s}^{(v)} \\ \hat{c}_{k,s}^{(c)} \end{bmatrix}, \quad (13)$$

Then it has been shown, that the diagonal part of Hamiltonian  $\hat{\mathcal{H}}_{\pi,t,\alpha_1}(u)$ , which corresponds to SSH one-electron treatment of electron-phonon coupling, can be represented in the form

$$\hat{\mathcal{H}}_{\pi,t,\alpha_1}^d(u) = \sum_k \sum_s 2\Delta_k \alpha_{k,s} \beta_{k,s} (\hat{n}_{k,s}^{(c)} - \hat{n}_{k,s}^{(v)}), \quad (14)$$

where  $\Delta_k = 4\alpha_1 u \sin ka$ ,  $\hat{n}_{k,s}^{(c)}$  is density of operator of quasiparticles' number in  $c$ -band,  $\hat{n}_{k,s}^{(v)}$  is density of operator of quasiparticles' number in  $v$ -band.

The diagonal part  $\hat{\mathcal{H}}_{\pi,u,\alpha_2}^d(u)$  of operator  $\hat{\mathcal{H}}_{\pi,u,\alpha_2}(u)$  of pairwise interaction, which is linear in displacement coordinate  $u$  and leads to participation of the phonons, is given by the expression

$$\begin{aligned} \hat{\mathcal{H}}_{\pi,u,\alpha_2}^d(u) &= 4\alpha_2 u \sum_k \sum_{k'} \sum_s \alpha_{k'} \beta_{k'} (\hat{n}_{k',s}^{(v)} - \hat{n}_{k',s}^{(c)}) \\ &\times \alpha_{k,s} \beta_{k,s} (\hat{n}_{k,s}^{(v)} - \hat{n}_{k,s}^{(c)}) \sin k'a \sin ka \end{aligned} \quad (15)$$

Let us remark, that the Hamiltonian  $\hat{\mathcal{H}}_{\pi,u,\alpha_2}(u)$  describes the attraction between the electrons, it can lead to formation of Cooper pairs in a  $\pi$ -subsystem and to superconductivity of both of usual  $s$ -wave type, described in [24], that is, with Cooper pairs in singlet  $S = 0$  state and with Cooper pairs in triplet  $S = 1$  state. It is like to well-known possibility of the formation of singlet and triplet excitons and it seems to be substantial conclusion being to be the key moment for coexistence of superconductivity and magnetic ordering. In fact, the new mechanism for superconductivity was proposed.

The diagonal part  $\hat{\mathcal{H}}_{\pi,t_0}^d(u)$  of operator  $\hat{\mathcal{H}}_{\pi,t_0}(u)$  in terms of operator variables  $\hat{a}_{k,s}^{(c)}$ ,  $\hat{a}_{k,s}^{(v)}$  is given by the relation

$$\hat{\mathcal{H}}_{\pi,t_0}^d(u) = \sum_k \sum_s \epsilon_k (\alpha_{k,s}^2 - \beta_{k,s}^2) (\hat{n}_{k,s}^{(c)} - \hat{n}_{k,s}^{(v)}), \quad (16)$$

where  $\epsilon_k = 2t_0 \cos ka$ .

The operator transformation for the  $\sigma$ -subsystem, analogous to (13) shows, that the Hamiltonian  $\hat{\mathcal{H}}_0(u)$  is invariant under given transformation, that is, it can be represented in the form, given by (6).

To find the values of elements of matrix in relation (13), the Hamiltonian  $\hat{\mathcal{H}}(u)$  has been tested for conditional extremum in dependence on the variables  $\alpha_k$ ,  $\beta_k$  with condition  $\alpha_{k,s}^2 + \beta_{k,s}^2 = 1$ .

Two values for the energy of quasiparticles, indicating on the possibility of formation of the quasiparticles of two kinds both in  $c$ -band and  $v$ -band have been obtained.

They are the following

$$\begin{aligned} E_k^{(c)}(u) &= \frac{Q^2 \Delta_k^2 - \epsilon_k^2}{\sqrt{\epsilon_k^2 + Q^2 \Delta_k^2}}, \\ E_k^{(v)}(u) &= \frac{\epsilon_k^2 - Q^2 \Delta_k^2}{\sqrt{\epsilon_k^2 + Q^2 \Delta_k^2}} \end{aligned} \quad (17)$$

and

$$\begin{aligned} E_k^{(c)}(u) &= \sqrt{\epsilon_k^2 + Q^2 \Delta_k^2}, \\ E_k^{(v)}(u) &= -\sqrt{\epsilon_k^2 + Q^2 \Delta_k^2} \end{aligned} \quad (18)$$

The factor  $Q$  is determined by relation

$$\left[1 + \frac{\alpha_2}{2\alpha_1} \sum_k \sum_s \frac{Q \Delta_k \sin ka}{\sqrt{\epsilon_k^2 + Q^2 \Delta_k^2}} (n_{k,s}^{(c)} - n_{k,s}^{(v)})\right] = Q, \quad (19)$$

where  $n_{k,s}^{(c)}$  is eigenvalue of density operator of quasiparticles' number in  $c$ -band,  $n_{k,s}^{(v)}$  is eigenvalue of density operator of quasiparticles' number in  $v$ -band. The quasiparticles with the energy, determined by (18) at  $Q = 1$  are the same quasiparticles, that were obtained in known SSH-model.

Sufficient conditions for the minimum of the functions  $E(\alpha_{k,s}, \beta_{k,s})$  were obtained by standard way, which was used also in [20]. It consist in that, that the second differential of the energy being to be the function of three variables  $\alpha_{k,s}$ ,  $\beta_{k,s}$  and  $\lambda_{k,s}$  has to be positively defined quadratic form. From the condition of positiveness of three principal minors of quadratic form coefficients the three sufficient conditions for the energy minimum have been obtained. Their analysis has showed, that SSH-like solution is inapplicable for the description of standard processes, passing near equilibrium state by any parameters [30]. The quasiparticles, described by SSH-like solution, can be created the only in strongly nonequilibrium state with inverse population of the levels in  $c$ - and  $v$ -bands. At the same time the solution, the energy of quasiparticles for which is determined by (17) can be realised both in near equilibrium and in strongly nonequilibrium states of the  $\pi$ -subsystem of t-PA, which is considered to be quantum Fermi liquid [30].

The continuum limit for the ground state energy of the t-PA chain with SSH-like quasiparticles will coincide with known solution [32], if to replace  $\Delta_k Q \rightarrow \Delta_k$ . The calculation of the ground state energy  $E_0^{[u]}(u)$  of the t-PA chain with quasiparticles' branch, which is stable near equilibrium by taking into account, that in ground state  $n_{k,s}^c = 0$ ,  $n_{k,s}^v = 1$ , in the continuum limit gives

$$E_0^{[u]}(u) = -\frac{2Na}{\pi} \int_0^{\frac{\pi}{2a}} \frac{(Q\Delta_k)^2 - \epsilon_k^2}{\sqrt{Q\Delta_k^2 + \epsilon_k^2}} dk + 2NKu^2. \quad (20)$$

Then, calculation of the integral results in the expression

$$\begin{aligned} E_0^{[u]}(u) &= \frac{4Nt_0}{\pi} \left\{ F\left(\frac{\pi}{2}, 1 - z^2\right) + \right. \\ &\left. \frac{1 + z^2}{1 - z^2} [E\left(\frac{\pi}{2}, 1 - z^2\right) - F\left(\frac{\pi}{2}, 1 - z^2\right)] \right\} + 2NKu^2, \end{aligned} \quad (21)$$

where  $z^2 = \frac{2Q\alpha_1 u}{t_0}$ ,  $F(\frac{\pi}{2}, 1 - z^2)$  is the complete elliptic integral of the first kind and  $E(\frac{\pi}{2}, 1 - z^2)$  is the complete elliptic integral of the second kind. Approximation of ground state energy at  $z \ll 1$  for the stable near equilibrium solution gives

$$\begin{aligned} E_0^{[u]}(u) &= N \left\{ \frac{4t_0}{\pi} - \frac{6}{\pi} \ln \frac{2t_0}{Q\alpha_1 u} \frac{4(Q\alpha_1)^2 u^2}{t_0} + \right. \\ &\left. \frac{28(Q\alpha_1)^2 u^2}{\pi t_0} + \dots \right\} + 2NKu^2. \end{aligned} \quad (22)$$

It is seen from (22), that the energy of quasiparticles, described by given solution, has the form of Coleman-Weinberg potential with two minima at the values of dimerization coordinate  $u_0$  and  $-u_0$  like to the energy of quasiparticles, described by SSH-solution. It is understandable, that further considerations, including electrically neutral  $S = 1/2$  soliton and electrically charged spinless soliton formation, that is the appearance of the phenomenon of spin-charge separation, by FL description of 1D systems will be coinciding in its mathematical form with those ones in SSH-model.

Thus, in [30] was established the possibility to describe the physical properties of 1D systems in the frames of 1D quantum FL including the mechanism of appearance of the most prominent feature of 1D systems - the phenomenon of spin-charge separation. It was also shown the possibility of simultaneous formation of superconducting state and the state with magnetic ordering in 1D FL.

Let us remark, that the model proposed takes into consideration the electron-electron correlations in explicit form, which seems to be ground for its application to electronic system of quasi-1D NTs, where electron-electron correlations are known to be rather strong. In particular, it can be used for analysis of ESR spectra. It can be done by above indicated manner, that is by using of hypercomplex number theory analogously to theoretical analysis of quantum optics effects in [22] and analysis in [20] of Raman spectra in quasi-1D NTs. It is essential, that the FL soliton spin-charge separation mechanism in quasi-1D carbon NTs has experimental confirmation [16], [19], [18], whereas the LL (FLL) spin-charge separation mechanism has not been found. It seems to be the direct confirmation of the applicability of the theory of FL above considered to carbon quasi-1D NTs. Given results mean, that the explanation of the results, presented in Section III, has to take into consideration the FL behavior of electronic system of NTs, incorporated in diamond single crystal in [100] direction. It is the main consequence of given part for the subsequent analysis. On the other hand, it justifies the brief representation of the results of the work [30].

The results above considered show, that the shape of  $\pi$ -solitons (or  $\sigma$ -solitons) is given by the expression with the same mathematical form both in SSH-model and in its FL generalization. It is

$$|\phi(n)|^2 = \frac{1}{\xi_{\pi(\sigma)}} \text{sech}^2 \left[ \frac{(n - n_0)a}{\xi_{\pi(\sigma)}} - v_{\pi(\sigma)} t \right] \cos^2 \frac{n\pi}{2}, \quad (23)$$

where  $n, n_0$  are, correspondingly, variable and fixed numbers of  $CH$ -unit in  $CH$ -chain,  $a$  is  $C - C$  interatomic spacing projection on chain direction,  $v_{\pi(\sigma)}$  is  $\pi$  ( $\sigma$ )-soliton velocity,  $t$  is time,  $\xi_{\pi(\sigma)}$  is  $\pi$  ( $\sigma$ ) coherence length. It is seen, that  $\pi$ -solitons ( $\sigma$ -solitons) differ in fact the only by numerical value of coherence length in SSH-model and in its FL generalization. Really, the coherence lengths  $\xi_{0\pi}$  and  $\xi_{0\sigma}$  are determined by the relation [33]

$$\xi_{0\pi} = \frac{\hbar v_F}{\Delta_{0\pi}}, \xi_{0\sigma} = \frac{\hbar v_F}{\Delta_{0\sigma}}, \quad (24)$$

where  $\Delta_{0\sigma}$ ,  $\Delta_{0\pi}$  are  $\sigma$ - and  $\pi$ -bandgap values at  $T = 0K$ ,  $v_F$  is Fermi velocity. In SSH-model  $v_F$  is proportional to  $t_0$ , in SSH-FL-model, here presented,  $v_F$  is proportional to sum  $t_0 + t_1$ . It allows to explain some discrepancy between theoretical value in SSH-model and experimental values for  $\xi_{\pi}$  and its dispersion, depending on production technology. Theoretical value in SSH-model for  $\xi_{\pi}$  in t-PA is  $7a$ , and it is low boundary in the range  $7a - 11a$ , obtained for  $\xi_{\pi}$  from experiments [34]. It means, that in the samples with  $\pi$ -soliton coherence length, equaled to  $11a$ ,  $t_1$  is equal to  $0.57t_0$  at the same t-PA band gap value (it is possible, since factor  $Q$  is independent on  $t_1$  and can be close to 1).

Consequently, we come to conclusion, that the constant component in Taylor expansion of electron-electron interaction potential with the term, proportional to  $t_1$ , is substantial and that the value of  $t_1$  can depend on the preparation technology.

Above described experimental results obtained by ESR study of NTs, formed in diamond single crystals in the result of the  $\langle 100 \rangle$  ion beam modification indicate, that for the correct description of NTs' properties the  $\sigma$ -electronic subsystem has to be taken into consideration. It follows immediately from the appearance of inherent magnetic symmetry directions, which are not coinciding with host lattice symmetry directions. From the other hand, the analysis of numerical values of  $g$ -factor and linewidth values, Figure 6, Figure 8, means, that magnetic interactions are strong and their strength values are comparable with the corresponding values in usual magnetic systems with unfilled inner shells. At the same time, it is shown in [23], that in the case, when magnetic ordering is determined the only by  $\pi$ -subsystem of the NTs, the magnetic interactions are relatively weak, magnetic ordering symmetry characteristics are governed by symmetry directions of surrounding diamond lattice (with accuracy of implantation direction relatively diamond lattice axes symmetry directions). It takes place in NTs produced by means of  $\langle 110 \rangle$  ion beam modification and  $\langle 111 \rangle$  ion

beam modification. It seems to be evident that by  $\langle 110 \rangle$  ion beam modification we have the case of strong anti-ferromagnetic (AFM) ordering. Really, the conclusion on just AFM ordering (but not ferromagnetic) is in agreement with observation of two both very broad and two moderately broad lines. The appearance of two AFM-resonance lines (if linearly polarised microwave field is used by detection, that was the case in our experiments) was established by Kittel in the work [35], which was the first work on the theory of AFM-resonance. It has been found in related our work [36], that magnetic moments of two sublattices being to be opposite directed are uncompensated in their magnitude, that is, strongly speaking, we are dealing with uncompensated AFM-resonance or, in other words, with ferrimagnetic resonance. This is so indeed, since the ratio of intensities of the absorption, corresponding to L and  $R_b$ -lines is equal to  $\approx 3.5$  [36].

Let us consider the following Hamiltonian

$$\hat{\mathcal{H}}(u) = \hat{\mathcal{H}}_0(u) + \hat{\mathcal{H}}_1(u) + \hat{\mathcal{H}}_2(u) + \hat{\mathcal{H}}_3(u) + \hat{\mathcal{H}}_4(u), \quad (25)$$

where  $u$  is configuration coordinate along the symmetry axis  $z$  of the individual chain of NT. It is suggested to be independent on site position and on subsystem kind. Operator  $\hat{\mathcal{H}}_0(u)$  is

$$\hat{\mathcal{H}}_0(u) = \sum_{\vec{k}} \sum_m \sum_q \sum_s \varepsilon^{mq}(u) \hat{c}_{\vec{k}ms}^+ \hat{c}_{\vec{k}qs}, \quad (26)$$

in which subscripts  $m, q = \{\pi, \sigma\}$ ,  $s$  is spin projection,  $\vec{k}$  is wave vector,  $\hat{c}_{\vec{k}ms}^+$ ,  $\hat{c}_{\vec{k}ms}$  are operators of creation and annihilation of the quasiparticle with spin projection  $s$  and wave vector  $\vec{k}$  in  $m$ th ( $q$ th) subsystem,  $\varepsilon^{mq}(u)$  are the resonance interaction integrals (hopping interaction in tight-binding model approximation) of quasiparticles in  $\pi$ -subsystem of electronic system, in  $\sigma$ -subsystem of electronic system, which are considered to be 1D quantum Fermi liquids, and between  $\pi$ - and  $\sigma$ -subsystems.

The operator  $\hat{\mathcal{H}}_1$  is

$$\hat{\mathcal{H}}_1(u) = \sum_m \sum_j U_1(j, m, u) \hat{c}_{jms(\uparrow)}^+ \hat{c}_{jms(\uparrow)} \hat{c}_{jms(\downarrow)}^+ \hat{c}_{jms(\downarrow)}, \quad (27)$$

where  $j = \overline{1, N}$  is the site position,  $U_1(j, m, u)$  is intrasubsystem Coulomb coupling parameter, which is dependent in general case on  $j, m, u$ . The operator  $\hat{\mathcal{H}}_2(u)$  is

$$\hat{\mathcal{H}}_2(u) = \sum_{m>q} \sum_j U_2(j, m, q, u) \sum_s \hat{c}_{jms}^+ \hat{c}_{jms} \sum_s \hat{c}_{jq s}^+ \hat{c}_{jq s} \quad (28)$$

where  $U_2(j, m, q, u)$  is intersubsystem Coulomb coupling parameter, which is dependent in general case on  $j, m, q, u$ . The operator  $\hat{\mathcal{H}}_3(u)$  is

$$\hat{\mathcal{H}}_3(u) = \sum_{m>q} \sum_j \sum_s \sum_{s'} J_1(j, m, q, u) \hat{c}_{jms}^+ \hat{c}_{jq s'}^+ \hat{c}_{jms'} \hat{c}_{jq s}, \quad (29)$$

where  $J_1(j, m, q, u)$  is the inter-subsystem Hund's rule coupling, which is dependent in general case on  $j, m, q, u$ .

The operator  $\hat{\mathcal{H}}_4(u)$  is

$$\hat{\mathcal{H}}_4 = \sum_{m \neq q} \sum_j J_2(j, m, q, u) \hat{c}_{jms(\uparrow)}^+ \hat{c}_{jms(\downarrow)}^+ \hat{c}_{jq s(\downarrow)} \hat{c}_{jq s(\uparrow)} \quad (30)$$

where  $J_2(j, m, q, u)$  is pair hopping parameter, which is dependent in general case on  $j, m, q, u$ .

Like to foregoing consideration the Hamiltonians  $\hat{\mathcal{H}}_1(u)$  and  $\hat{\mathcal{H}}_2(u)$  can be expanded in Taylor series about the dimerized state. So, restricting by two first terms in Taylor expansion, we have

$$\begin{aligned} \hat{\mathcal{H}}_1(u) = & \sum_m \sum_j (U_1^{(0)} + \\ & (-1)^j 2\alpha_1^m u) \hat{c}_{jms(\uparrow)}^+ \hat{c}_{jms(\uparrow)} \hat{c}_{jms(\downarrow)}^+ \hat{c}_{jms(\downarrow)}, \end{aligned} \quad (31)$$

where  $\{\alpha_1^m\}$ ,  $m = \{\pi, \sigma\}$  are constants of electron-phonon interactions, accompanying the processes of intrasubsystem Coulomb interactions.

$$\begin{aligned} \hat{\mathcal{H}}_2(u) = & \sum_{m > q} \sum_j (U_2^{(0)} + \\ & (-1)^j 2\alpha_2^{mq} u) \sum_s \hat{c}_{jms}^+ \hat{c}_{jms} \sum_s \hat{c}_{jq s}^+ \hat{c}_{jq s}, \end{aligned} \quad (32)$$

where  $\{\alpha_2^{mq}\}$ ,  $m, q = \{\pi, \sigma\}$  are constants of electron-phonon interactions, accompanying the processes of intersubsystem Coulomb interactions. It is clear, that the second terms in (31) and in (32) describe the attraction between strongly correlated electrons, it can explain the nature of the pairing mechanism in high temperature superconductors.

The Hamiltonian  $\hat{\mathcal{H}}(u)$  can be considered to be basic Hamiltonian for its generalization to describe the properties of carbon NTs, produced by  $\langle 100 \rangle$  ion beam modification of diamond single crystals, in particular for analysis of ESR data above described. The generalization of the Hamiltonian  $\hat{\mathcal{H}}(u)$  can be done by the way, proposed in [22] on the basis of hypercomplex number theory, at that it has to be taken into account, that, strongly speaking, NTs, produced by  $\langle 100 \rangle$  implantation can be described in the framework of hypercomplex number theory by its generalization too, since  $C_4$  symmetry indicates on inequivalence of the chains along the NT axis.

Let us remark, that the Hamiltonian (25) is similar to two-orbital-Hamiltonian, proposed in [37] for spectral analysis of the iron-based superconductors. It will be almost coinciding in the case when  $\{\alpha_1^m\} = 0$ ,  $m = \{\pi, \sigma\}$ ,  $\{\alpha_2^{mq}\} = 0$ ,  $m, q = \{\pi, \sigma\}$ ,  $J_1(j, m, q, u)$ ,  $J_2(j, m, q, u)$  are independent on  $j, m, q, u$ . The difference in given case consists in inequivalence of  $\sigma$  and  $\pi$ -subsystems, in comparison with equivalence of Fe orbitals  $d_{xz}$  and  $d_{yz}$ , considered in [37]. However, even in given more simple case the task was solved the only by numerical methods. The main result is represented in Figure 8 in [37].

The magnetic excitation spectrum carries information on the nature of magnetism and the characteristics of superconductivity. It has been discussed in the literature, that an observation of a sharp quasiparticle-like

resonance peak in the spin fluctuation spectrum with the onset of superconductivity may strongly indicate a sign change in the gap structure caused by the superconducting coherence factors. It has been established, that in iron pnictides a strong spin resonance occurs in the  $s^+$ -wave SSt. The comparison of the ESR spectra, Figures 1 to 3, with theoretically calculated spectral function, presented in Figure 8 in [37] allows to suggest, that the spontaneous transition in ESR response in the sample studied indicates on transition to SSt-state, which is coexisting with antiferromagnetic ordering. Therefore, it is additional confirmation, that two lines - L-line and  $R_b$ -line - are assigned with AFM-resonance observed in SSt-state. Inequivalence of the main characteristics of given lines can be attributed to strong inequivalence of two subsystems in NTs in comparison with theoretically calculated in [37]. It seems to be essential the result in given work indicating on the appearance of absorption with very broad spectral distribution and peak-dip-hump feature when the system becomes superconducting. We have observed the derivative of spectral function, which corresponds by its integration to spectral function with two peak-dip-hump features. It seems to be consequence of different coupling of the resonance mode to fermions in  $\pi$  and  $\sigma$ -subsystems. Spectral function, presented in Figure 8 in [37], was calculated numerically and physical nature of the appearance of absorption with very broad spectral distribution has not been established. It has been done in the work [38]. The authors have been studied theoretically the spin response in the normal and superconducting states of Fe-based pnictide superconductors. They showed that the resulting magnetic fluctuation spectrum calculated within random-phase approximation consists of two contributions. The first contribution is determined by the antiferromagnetic spin fluctuations peaked at wave vector  $\vec{Q}_{AFM}$  arising in the result of the interband scattering. The second contribution comes from the intraband scattering and results in a broad continuum of the SDW fluctuations with a small momenta.

Further the authors of [37] indicate, that "detailed study of the magnetic and the electronic spectrum shows that the dispersion of the magnetic resonance mode in the nearly isotropic  $s^+$  superconducting state exhibits anisotropic propagating behavior in an upward pattern". Given conclusion is also in agreement with experiment [36].

Further, the observation of superlinear dependence in absorption kinetics, corresponding to L-line, Figure 4, is strong evidence of the mobility of spin carriers [19]. The switching from the saturating behavior to nonsaturating behavior with superlinear absorption kinetics of  $R_b$ -line, Figure 5, can be attributed to decrease of screening of microwave magnetic field (and static magnetic field too) by  $\pi$  subsystem when microwave power is increased in the range  $H_1/H_1^{(0)} 0.75 - 1$ . Here we take in mind the reasonable suggestion that screening effect by  $\pi$  subsystem is substantially more strong in comparison with screening effect by  $\sigma$ -subsystem and microwave field pen-

etrates more effectively at low microwave power through  $\sigma$ -subsystem. In fact, the spin carriers in  $\pi$  subsystem are pinned at low power, it is the consequence of short penetration depth. Sharp increase of absorption in the range  $H_1/H_1^{(0)} 0.75 - 1$  is explained then by two factors - by depinning and by increasing of the number of spin carriers, interacting with microwave field in given range.

In the favour of the SSt formation indicates the observation of Dyson-like effect with unusual angular dependence of asymmetry extent A/B of L-line. It is qualitatively explained in [36]. It seems to be also understandable the presence of some angular dependence of Q-factor. It is seen from Figure 10, that relative change of Q-factor is small (although it is surely detectable), Q-factor is nonmonotonically increased by the change of sample rotation angle from [011] to [100] the only in 1.115 times. Some decrease of Q-factor in the range (60 - 90) degrees from [100] can be explained by the existence of nonsuperconducting part of NT-network, [which is confirmed by the detection of practically isotropic narrow line  $R_n$ ] at simultaneous decrease of the contribution in the total superconducting state of intraband transitions (see for details further), detected by very broad lines, which is decreasing in given range (corresponding Figures are not represented). In other words, in given range the redistribution of resonance absorption contribution between superconducting and nonsuperconducting parts in the favour of nonsuperconducting part, which characterises by some cavity Q-losses, although they are small, takes place. The fact, that the maximal Q-factor value is achieved in [100] direction can be explained in the following way. In given direction the part of microwave power can penetrate through free unmodified diamond space between NTs to all sample volume, which is insulating and it is free from any magnetic impurities. That means, that the relative contribution of nonsuperconducting part of NT-network with some small Q-losses into total resonance and nonresonance parts of the interaction of all sample electronic subsystems with microwave field has to be minimal, which is really observed.

The very pronounced angular dependence of linewidth of L-line seems to be the most clear demonstration of Meissner effect. Meissner effect is expected to be very anisotropic in the sample studied, since, on the one hand, the superconductivity is suggested to be multichannel (see further), that is, it is determined by different mechanisms simultaneously. On the other hand, there are in the sample unmodified regions between NTs in NT-network, which strengthen anisotropy of Meissner effect. So, near the [100] direction Meissner effect seems to be minimal, since static magnetic field  $H_0$  can penetrate along NT axes both in inner NT space and in outer surrounding unmodified diamond regions. That ensures the minimal inhomogeneity of magnetic field along all tube surface and minimal value of linewidth, which really takes place. In other words, effective thickness of superconducting layer seems to be less than penetration depth value in Meissner effect. Then, the linewidth increase, which is start-

ing from 5 degrees [given value is the only approximate value, more precise measurements were not provided] by increase of effective thickness of superconducting layer, since individual static magnetic field line will intersect the big number of NTs even by small deviation from strict implantation direction. Let us remark, that our previous measurements show, that inaccuracy in implantation direction by implantation process does not exceed 1 degree, at the same time we have to remark, that some inaccuracy can be in given experiment in determination of [100] direction in sample rotation plane (which, however does not exceed 2 degrees). Then the appearance of branch in (5-40) degree range, where the growth of linewidth of line L is observed, is explained by inhomogeneity increase along individual static magnetic field line determined by Meissner effect. Given viewpoint correlates well with data on angular dependence of absorption intensity. It is seen from Figure 7, that growth of absorption intensity in (5-40) degree range is not pronounced, since, although the effective thickness of operating region for absorption process is increased, but inhomogeneity of amplitude of magnetic component of microwave field is also increased, being to be the consequence of Meissner effect too. In fact, the average value of amplitude of magnetic component  $H_1$  of microwave field is decreased, resulting in almost compensation of effect of growth of effective thickness of absorbing layer. Starting from 40 degrees upto  $\approx 70$  degrees the processes of intraband transitions become very effective [in AFM channel the very broad lines are corresponding to given processes, it really takes place, the corresponding Figures are not represented, although the readers can compare the Figures 2 and 3 with the Figure 1]. It leads to substantial decrease of penetration depth, resulting in substantial decrease of the effective thickness of absorbing layer. It means, that part of NTs along individual static magnetic field line drop out from resonance conditions at all, being to be consequence of screening both static magnetic field and microwave field. It is understandable, that both absorption intensity and linewidth of line L have to be decreasing, at that the appearance of absorption intensity decreasing is evident (both average value of  $H_1$  and effective number of absorbing spin carriers are decreasing). Linewidth decreasing is explained by decrease of range of static magnetic field, where resonance conditions can be restored by  $H_0$  scan, being to be consequence on more sharp  $H_0$ -field strength damping to the same near zero value. Given conclusions correspond to experimental data, see Figures 7 and 8. The second branch of linewidth growth, starting in the range 70-75 degrees from [100] direction, Figure 8, and corresponding branch of intensity growth, Figure 7, have the same origin, which has linewidth and absorption intensity growth, starting at  $\approx 5$  degrees. It is direct consequence of the damping of intraband transitions, taking place in given range. It explains the resemblance of two branches of linewidth growth, starting at  $\approx 5$  degrees and in the range 70-75 degrees from [100] direction, seen in Figure 8. The difference of analogous branches of ab-



sorption intensity growth can be explained by different screening of magnetic component  $H_1$  of microwave field in given ranges. Actually, when  $H_0$  is near [100] direction, then propagation direction for microwave field is near [011] direction, that is, near the direction, which is transverse to tube axes. Given direction is characterised by strong reflection and backscattering of microwave power. At the same time, when  $H_0$  is near [011] direction, then propagation direction for microwave field is near [100] direction, that is, near the direction, which is parallel to tube axes. In given case reflection and backscattering of microwave power leads to its propagation along NT surface in intertube space.

Therefore, the observed angular dependences of linewidth of line L and absorption intensity, corresponding to given line, become clear qualitative explanation by taking into consideration the Meissner effect.

Let us give some simple evaluation of penetration depth, based on given experimental results. The effective diameter of NTs can be evaluated from near surface layer modification extent with ion beam dose increase. It was surely established in previous studies, see, for instance, [20] that at  $5 \times 10^{14} \text{ cm}^{-2}$  ion integral fluence the entire modification takes place. Then in the approximation of uniform tube distribution and by neglecting of track canneling, we obtain the diameter value, equal to  $\approx 4.5 \text{ \AA}$ . The effective distance between NT centers by the same suggestions at  $5 \times 10^{13} \text{ cm}^{-2}$  ion integral fluence is  $\approx 14 \text{ \AA}$ . Then assuming that by direction in 5 degrees intersection length by individual static magnetic field line is achieved the penetration depth value, we obtain the number of the NTs intersected, equal to  $\approx 2500$  [The length of superconducting part of NT was taken to be equal  $20 \text{ }\mu\text{m}$ . Although the strict value of the ratio of the lengths of superconducting and nonsuperconducting parts is unknown, given value seems to be suitable for approximate evaluation.] Then by using of effective superconducting depth for individual NT, equal to interatomic distance in graphene layer, that is  $1.42 \text{ \AA}$  instead of intertube distance we obtain the value of penetration depth in  $\approx 34 \text{ nm}$ . Naturally, given evaluation gives the only order for penetration depth value, however given evaluation is coinciding in its order with well known penetration depth, in particular, with Londons' length, which is equal to (in its order)  $\sim 10 \text{ nm}$  in superconducting metals.

Let us represent some additional arguments in favour of the interpretation above proposed. The very strong additional argument is the observation of very pronounced Dyson-like effect itself, which, what is more, is observed by unconventional A/B angular dependence. For comparison, in very similar NT-system, which was formed inside the channels of a non-magnetic insulating SAPO 5 zeolite crystal Dyson effect was not observed [39]. Let us give a detailed description of given system preparation. According to [39] the sample preparation method involves heat treatment of a SAPO 5 in an inert atmosphere (pyrolysis) and filling its pores with a suitable car-

bon source. It results in the presence of the NTs with the only three chiralities (5,0) (4,2) and (3,3), thus minimizing chiral distribution. It has also been inferred that (5,0) and (3,3) chiral tubes are metallic (it seems to be essential for comparison with our results) and (4,2) tubes are semiconducting. Raman radial breathing mode (RBM) features indicate an average inner diameter of  $0.4 \text{ nm}$  for given single walled carbon nanotubes. From the optical polarized photoluminescence data, the arrays of SWNTs are found to align according to the channels of the zeolite crystal. The ESR samples studied in [39] imply that single walled carbon nanotubes are occluded inside the channels of a non-magnetic insulating SAPO 5 zeolite crystal. For reasons of comparison, ESR observations have also been carried out on free standing SWCNTs obtained through dissolution of the zeolite matrix in aqueous acidic solution. At all the temperatures covered, a symmetric isotropic ESR signal was observed at zero-crossing g-value  $g_c \approx 2.0025$ , indicating on the absence of Dyson effect.

Given comparison seems to be correct since track surface is in fact SWCNT, at that the diameter of NTs is also comparable. Let us remark once again, that two kinds of SWCNTs in [39] were identified to be metallic. Therefore, even given comparison seems to be sufficient to confirm the conclusion on the reality of AFM-SSt of NTs in our sample, since to observe Dyson-like effect the conductivity has to be better than metallic.

To explain the symmetry character of angular dependence of strong absorption with very broad lines, let us consider the band model of NTs. For qualitative conclusions, it seems to be sufficient to consider the band model of graphene.

The first calculation of electronic states in a 2D lattice of carbon atoms with a honeycomb symmetry have been undertaken by Wallace [40] in 1947. Wallace used graphene to be a starting element for description of bands in bulk graphite. Taking into account the strong hybridization of  $2s2p^2$  orbitals in the graphene plane, Wallace considered just the remaining  $p$  orbital (oriented perpendicular to the crystal plane) to be responsible for the electronic band structure in the vicinity of the Fermi level and suggested a standard tight-binding approach. Considering the only the nearest-neighbour hopping parameter  $\gamma_0$ , a pair of  $\pi$ -bands is obtained [41]

$$E_{\pi}^*(\vec{k}) = -E_{\pi}(\vec{k}) = \gamma_0 \sqrt{1 + 4 \cos^2 \frac{4k_y a_0}{2} + 4 \cos \frac{4k_x \sqrt{3} a_0}{2} \cos \frac{4k_y a_0}{2}}, \quad (33)$$

which distinctly cross (touch) at two inequivalent  $K$  and  $K'$  points of the Brillouin zone. The strength of the nearest-neighbour hopping is  $3.2 \text{ eV}$  and the lattice constant  $a_0 = 0.246 \text{ nm}$  is by a factor of  $\sqrt{3}$  larger than the distance between the nearest carbon atoms.

So, in pristine graphene, the Fermi level lies just at the touching (crossing) point (the Dirac or charge neutrality

point) of  $\pi^*$  and  $\pi$  bands and graphene has a character of zero-band-gap semiconductor (semimetal). Band structure on some distance from Fermi level consist of six symmetric Dirac cones in the approach above considered, with vertices, which produce regular hexagon, that is with angle distance from each other in  $\pi/3$  relatively the hexagon center. To the first approximation given structure is retained for NTs, that seems to be substantial for the explanation of the observed experimental data in  $\langle 100 \rangle$ -incorporated NTs, which are displaying own symmetry, different from diamond lattice symmetry (see further).

Close to a given crossing (touching) point, the electronic bands are nearly linear and practically rotationally symmetric. In other words, the carrier dispersion relations take a simple form

$$E_\pi^* = -E_\pi \approx v_F \hbar |\vec{k}|, \quad (34)$$

where the momentum  $\vec{k}$  is measured with respect to  $K(K')$  point. The parameter  $v_F$ , having dimension of a velocity, is directly related to the coupling strength (hopping integral) between the nearest carbon atoms:  $v_F = \sqrt{3}a_0\gamma_0/(2\hbar)$ . It is known, that the linearity of bands in graphene (in the vicinity of the  $K$  and  $K'$  points) implies, on the one hand, that charge carriers behavior in pristine graphene is like to relativistic particles with zero rest mass and constant velocity  $v_F$ , equaled to  $\approx 10^6 \text{ cm s}^{-1}$  in given case. They are often attributed to massless Dirac fermions, and their behaviour is described by the effective Hamiltonian [41]

$$\hat{H} = v_F \begin{bmatrix} 0 & \hat{p}_x - i\hat{p}_y \\ \hat{p}_x + i\hat{p}_y & 0 \end{bmatrix} = v_F \hat{\sigma} \hat{p}, \quad (35)$$

which is equivalent to the Hamiltonian in the Weyl equation for real relativistic particles with zero rest mass (originally for neutrinos) derived from the Dirac equation. On the other hand, the dispersion relation (34) is key relation for LL-behavior of electronic system. Therefore, in the first approximation the electronic system of graphene is considered in the literature to be 2D-Luttinger liquid system, which seems to be incorrect, taking into account foregoing discussion.

Therefore, the relativistic-like image of electronic states in graphene given by Hamiltonian (35) remains to our opinion an very approximate model. Even in the case of electronic states in the vicinity of the Dirac point the interaction with phonon subsystem has to be taken into consideration. It can lead qualitatively to the same simple model proposed, however numerical characteristics will be other. Naturally, the deviations from this relativistic model become significant for states far away from the Dirac point, even if only the nearest neighbours in the tight-binding calculation are considered. Other deviations may arise when including the hopping integrals between next-nearest neighbours. For example, when taking into account the non-zero values of next-nearest hopping integrals, the nonlinearity is enhanced and Dirac

cones become asymmetric with respect to the charge neutrality point.

Qualitatively the characteristic features of angular dependencies of the parameters of ESR-spectra observed can be explained now in the following way. The quasi-particle spectral function, which describes the ESR spectrum observed is [37]

$$A(\vec{k}, \omega) = -\frac{1}{\pi} \text{Im} \left[ \sum_a G^{aa}(\vec{k}, i\omega_n \rightarrow \omega + i\delta) \right] \quad (36)$$

with the dressed normal single-particle propagators  $G^{aa}$  determined by solving the coupled Dyson-Gorkov's equations,  $\omega_n$  is bosonic Matsubara frequency,  $\omega_n = 2n\pi T$ . We see, that spectral function depend on  $\vec{k}$  in explicit form. The value of AFM vector  $\vec{Q}$  is determined by  $\vec{k}$ -differences between inequivalent  $K$  and  $K'$  points of Dirac cones, that is by  $\pi/3$ , which is really experimentally displaying in angular dependencies of absorption spectral distribution. In particular, it becomes to be understandable, why the absorption with very broad two lines is observed in the range of the angles near  $\pi/3$  with intensity maximum at  $\pi/3$  and coincidence of peak-dip-hump features of both very broad lines at given angle. It is taken into account, that periodical function in wave vector  $k$ -space has the main mode with the same period in frequency  $\omega$ -space, which is equivalent to  $H_0$  space, realized by scanning of static magnetic field, by means of which the spectra were registered.

We see from foregoing theoretical consideration, that in the case considered the advantages of several mechanisms of SSF formation can be joined. On the one hand, s-wave mechanism, mediated by the coupling of charge carriers with stretched phonon modes like to  $MgB_2$ , heavily boron doped diamond and sandwich S-Si-QW-S structures can be taking place. Moreover, just crimped cylindrical shape allows to increase the strength of C-C bonds by preservation of high density of the states on FS, resulting from low dimensionality (which seems to be intermediate between 1D and 2D). On the other hand, the multiband structure of valence and conductivity bands allows to realise the formation of AFM-SSF by means of the  $s^+$ -wave formation like to pnictides and additionally  $p$ -wave formation. It seems to be new mechanism - joint  $s^+$ - $p$ -wave mechanism. Just given mechanism is experimentally proved. The independent on dimerization coordinate (which can be both in static and dynamic states) electron-electron repulsion term can give the contribution to AFM-SSF formation by given mechanism. The foregoing theoretical consideration allow to suggest also, that usual s-wave BCS mechanism with  $S = 0$  Cooper pairing process of quasiparticles can produce additional independent superconducting channel. Given mechanism cannot be detected, however, by magnetic resonance technique directly. Along with given mechanism, the s-wave BCS-like mechanism with  $S = 1$  Cooper pairing process of quasiparticles can in principle also take place. The attractive terms, which are proportional to dimerization

coordinate, seem to be contributing to given phonon-mediated mechanisms and to  $s$ -wave mechanisms, mediated by the coupling of charge carriers with stretched phonon modes like to those ones established in  $MgB_2$ , heavily boron doped diamond and sandwich S-Si-QW-S structures. Further, the formation of  $\sigma$ -polaron lattice with AFM-ordering, which takes place, for instance in the samples, implanted in  $\langle 111 \rangle$  direction [20], leads also to new possible mechanism of AFM-SSt formation. It will be pure  $s^+$ -wave mechanism, like to those taking place in many pnictides. Main feature, which differ given mechanism from known ones is the other spatial distribution of delocalised spins. It is  $\sigma$ -polaron lattice instead SDW.

Therefore, all the terms in Taylor expansion of electron-electron interaction above considered can contribute to formation of SSt by different channels.

The switch to the SSt allows to explain the substantial broadening of ESR-lines, both, the rather large minimal value of the linewidth of  $L$ -line and  $R_b$ -line in comparison with  $R_n$ -line in nonsuperconducting state, which seems to be partly coexisting in the sample studied (let us remember, that it is indicated by the presence of  $R_n$ -line in ESR-spectra). Really, in the SSt with a momentum dependent SSt-gap ESR linewidth  $\Delta H$  is determined by spin-lattice relaxation time  $T_1$ ,  $\Delta H \sim 1/T_1$ , which is generally given by (see, for instance, [42])

$$\frac{(T_1 T)^{-1}}{(T_1 T)_{T=T_c}^{-1}} = \frac{2}{k_B T_c} \int_0^\infty [N_s^2(E) + \alpha_c M_s^2(E)] f(E) [1 - f(E)] dE, \quad (37)$$

where

$$N_s(E) = \frac{1}{4\pi} \int_0^{2\pi} \int_0^\pi \frac{E}{\sqrt{E^2 - |\Delta(\phi, \theta)|^2}} \sin \theta d\phi d\theta \quad (38)$$

$$M_s(E) = \frac{1}{4\pi} \int_0^{2\pi} \int_0^\pi \frac{|\Delta(\phi, \theta)|}{\sqrt{E^2 - |\Delta(\phi, \theta)|^2}} \sin \theta d\phi d\theta, \quad (39)$$

$N_s(E)$  and  $M_s(E)$  are the density of states (DOS) for quasiparticles and the anomalous DOS originating from the coherence effect of the transition probability in the SSt, respectively,  $\Delta(\phi, \theta)$  is SSt-gap. In conventional  $s$ -wave SSt, the presence of  $M_s(E)$  gives rise to  $\Delta H$  just below  $T_c$  since it usually has an isotropic gap with the same sign on the all Fermi surfaces. By contrast, in unconventional  $d$ -wave and/or  $p$ -wave SSt-states, the  $M_s(E)$  term is cancelled out by integrating over the momentum space on the SSt-gap. It can explain the difference in linewidth values for  $L$ - and  $R_b$  lines, which seems to be connected with  $s$ - and  $p$ -wave SSts correspondingly, simultaneously realized in the sample studied. In the multiband system, the  $N_s(E)$  and  $M_s(E)$  terms in

(37) are represented in the form  $(N_s^h(E) + N_s^e(E))$  and  $(M_s^h(E) + M_s^e(E))$ , respectively, where the  $N_s^h(E)$  and  $N_s^e(E)$  are the DOS of the hole and electron FSs, respectively. In the case of the Fe-pnictides the  $M_s(E)$  is negligibly small. It was theoretically proposed that this result is accounted for on a basis of a nodeless  $s^+$ -wave pairing scenario assuming a sign reversal gap function,  $+\Delta_h$  and  $-\Delta_e$  on the hole and electron FSs, respectively. In cases, where the  $\Delta_h$  and  $\Delta_e$  have opposite signs, it is noteworthy that the  $2M_s^h(E) \times M_s^e(E)$  component in  $(M_s^h(E) + M_s^e(E))^2$  becomes negative. In particular, when assuming the well-nested FSs, it is anticipated that the sign-nonconserving interband scattering process ( $+\Delta_h \leftrightarrow -\Delta_e$ ) may exceed the sign-conserving intraband scattering process ( $+\Delta_h \leftrightarrow +\Delta_h$  and  $\Delta_e \leftrightarrow \Delta_e$ ). The former process reduces the  $M_s^2(E)$  term through the negative contribution of the  $2M_s^h(E) \times M_s^e(E)$ , whereas the latter process does not. Here, to deal with convoluted intraband and interband contributions in the spin relaxation process the coefficient  $\alpha_c$  in expression (37) is introduced phenomenologically. It takes a value  $\alpha_c \leq 1$  depending on the weight of the interband contribution. Really, the substantial increase of linewidth  $L$  in AFM-SC state in comparison with  $R_n$ -line means, that coefficient  $\alpha_c$  in (37) is nonzero. Moreover, increase of linewidth of  $R_b$ -line in comparison with  $R_n$ -line means, that there is the additional mechanism of line broadening in addition to above considered. It is determined by Meissner effect and always will be take place by transition to SSt independently on superconductivity mechanism.

More detailed studies are necessary to clarify all the processes leading to room temperature superconductivity. In particular, all known models cannot explain the observation of the transition to AFM-SSt just in magnetic spin resonance conditions. To explain the role of spin resonance conditions for switch to AFM-SSt we have to take into account the quantum nature of EM-field in radiospectroscopy range. Given task has been solved in [43], where matrix-operator difference-differential equations for dynamics of spectroscopic transitions in 1D multiqubit exchange coupled (para)magnetic and optical systems by strong dipole-photon and dipole-phonon coupling are derived within the framework of quantum field theory. It has been established, that in the model considered the relaxation processes are of pure quantum character, which is determined by the formation of the coherent system of the resonance phonons and by the appearance along with absorption process of EM-field energy the coherent emission process, accompanying by phonon Rabi quantum oscillations, which can be time-shared. For the case of radiospectroscopy it corresponds to the possibility of the simultaneous observation along with (para)magnetic spin resonance the acoustic spin resonance.

Let us represent the brief review for given results with the same aim, that is, for convenience of readers. In the work [44] the system of difference-differential equations for dynamics of spectroscopic transitions for both radio-

and optical spectroscopy for the model, representing itself the 1D-chain of  $N$  two-level equivalent elements coupled by exchange interaction (or its optical analogue for the optical transitions) between themselves and interacting with quantized EM-field and quantized phonon field has recently been derived. The model presented in [44] differs from Tavis-Cummings model [45] the most essentially by inclusion into consideration of quantized phonon system, describing the relaxation processes from quantum field theory position. Seven equations for the seven operator variables, describing joint system {field + matter} were presented in matrix form by three matrix equations. They are the following

$$\frac{\partial}{\partial t} \begin{bmatrix} \hat{\sigma}_l^- \\ \hat{\sigma}_l^+ \\ \hat{\sigma}_l^z \end{bmatrix} = 2 \|g\| \begin{bmatrix} \hat{F}_l^- \\ \hat{F}_l^+ \\ \hat{F}_l^z \end{bmatrix} + \|\hat{R}_{\vec{q}l}^{(\lambda)}\|, \quad (40)$$

$$\begin{aligned} \frac{\partial}{\partial t} \begin{bmatrix} \hat{a}_{\vec{k}} \\ \hat{a}_{\vec{k}}^+ \end{bmatrix} &= -i\omega_{\vec{k}} \|\sigma_P^z\| \begin{bmatrix} \hat{a}_{\vec{k}} \\ \hat{a}_{\vec{k}}^+ \end{bmatrix} \\ &+ \frac{i}{\hbar} \begin{bmatrix} -\sum_{l=1}^N (\hat{\sigma}_l^+ + \hat{\sigma}_l^-) v_{l\vec{k}}^* \\ \sum_{l=1}^N (\hat{\sigma}_l^+ + \hat{\sigma}_l^-) v_{l\vec{k}} \end{bmatrix}, \end{aligned} \quad (41)$$

$$\begin{aligned} \frac{\partial}{\partial t} \begin{bmatrix} \hat{b}_{\vec{k}} \\ \hat{b}_{\vec{q}}^+ \end{bmatrix} &= -i\omega_{\vec{q}} \|\sigma_P^z\| \begin{bmatrix} \hat{b}_{\vec{q}} \\ \hat{b}_{\vec{q}}^+ \end{bmatrix} + \\ &\frac{i}{\hbar} \begin{bmatrix} -\sum_{l=1}^N \hat{\sigma}_l^z \lambda_{\vec{q}l} \\ \sum_{l=1}^N \hat{\sigma}_l^z \lambda_{\vec{q}l} \end{bmatrix}, \end{aligned} \quad (42)$$

where

$$\begin{bmatrix} \hat{\sigma}_l^- \\ \hat{\sigma}_l^+ \\ \hat{\sigma}_l^z \end{bmatrix} = \hat{\sigma}_l = \hat{\sigma}_l^- \vec{e}_+ + \hat{\sigma}_l^+ \vec{e}_- + \hat{\sigma}_l^z \vec{e}_z \quad (43)$$

is vector-operator of spectroscopic transitions for  $l$ th chain unit,  $l = \overline{2, N-1}$  [44]. Its components, that is, the operators

$$\hat{\sigma}_v^{jm} \equiv |j_v\rangle \langle m_v| \quad (44)$$

are set up in correspondence to the states  $|j_v\rangle, \langle m_v|$ , where  $v = \overline{1, N}$ ,  $j = \alpha, \beta$ ,  $m = \alpha, \beta$ . For instance, the relationships for commutation rules are

$$[\hat{\sigma}_v^{lm}, \hat{\sigma}_v^{pq}] = \hat{\sigma}_v^{lq} \delta_{mp} - \hat{\sigma}_v^{pm} \delta_{ql}. \quad (45)$$

Further

$$\begin{bmatrix} \hat{F}_l^- \\ \hat{F}_l^+ \\ \hat{F}_l^z \end{bmatrix} = \hat{\vec{F}} = [\hat{\sigma}_l \otimes \hat{\vec{g}}_{l-1, l+1}], \quad (46)$$

where vector operators  $\hat{\vec{g}}_{l-1, l+1}$ ,  $l = \overline{2, N-1}$ , are given by the expressions

$$\hat{\vec{g}}_{l-1, l+1} = \hat{\vec{g}}_{l-1, l+1}^- \vec{e}_+ + \hat{\vec{g}}_{l-1, l+1}^+ \vec{e}_- + \hat{\vec{g}}_{l-1, l+1}^z \vec{e}_z, \quad (47)$$

in which

$$\hat{\vec{g}}_{l-1, l+1}^- = -\frac{1}{\hbar} \sum_{\vec{k}} \hat{f}_{l\vec{k}} - \frac{J}{\hbar} (\hat{\sigma}_{l+1}^- + \hat{\sigma}_{l-1}^-), \quad (48a)$$

$$\hat{\vec{g}}_{l-1, l+1}^+ = -\frac{1}{\hbar} \sum_{\vec{k}} \hat{f}_{l\vec{k}} - \frac{J}{\hbar} (\hat{\sigma}_{l+1}^+ + \hat{\sigma}_{l-1}^+), \quad (48b)$$

$$\hat{\vec{g}}_{l-1, l+1}^z = -\omega_l - \frac{J}{\hbar} (\hat{\sigma}_{l+1}^z + \hat{\sigma}_{l-1}^z). \quad (48c)$$

Here operator  $\hat{f}_{l\vec{k}}$  is

$$\hat{f}_{l\vec{k}} = v_{l\vec{k}} \hat{a}_{\vec{k}} + \hat{a}_{\vec{k}}^+ v_{l\vec{k}}^*. \quad (49)$$

In relations (48)  $J$  is the exchange interaction constant in the case of magnetic resonance transitions or its optical analogue in the case of optical transitions, the function  $v_{l\vec{k}}$  in (49) is

$$v_{l\vec{k}} = -\frac{1}{\hbar} p_l^{jm} (\vec{e}_{\vec{k}} \cdot \vec{e}_{\vec{P}_l}) \mathfrak{E}_{\vec{k}} e^{-i\omega_{\vec{k}} t + i\vec{k}\vec{r}}, \quad (50)$$

where  $p_l^{jm}$  is matrix element of operator of magnetic (electric) dipole moment  $\vec{P}_l$  of  $l$ -th chain unit between the states  $|j_l\rangle$  and  $|m_l\rangle$  with  $j \in \{\alpha, \beta\}$ ,  $m \in \{\alpha, \beta\}$ ,  $j \neq m$ ,  $\vec{e}_{\vec{k}}$  is unit polarization vector,  $\vec{e}_{\vec{P}_l}$  is unit vector along  $\vec{P}_l$ -direction,  $\mathfrak{E}_{\vec{k}}$  is the quantity, which has the dimension of magnetic (electric) field strength,  $\vec{k}$  is quantized EM-field wave vector, the components of which get a discrete set of values,  $\omega_{\vec{k}}$  is the frequency, corresponding to  $\vec{k}$ th mode of EM-field,  $\hat{a}_{\vec{k}}^+$  and  $\hat{a}_{\vec{k}}$  are EM-field creation and annihilation operators correspondingly. In the suggestion, that the contribution of spontaneous emission is relatively small,  $p_l^{jm} = p_l^{mj} \equiv p_l$ , where  $j \in \{\alpha, \beta\}$ ,  $m \in \{\alpha, \beta\}$ ,  $j \neq m$ . Further, matrix  $\|\hat{R}_{\vec{q}l}^{(\lambda)}\|$  is

$$\|\hat{R}_{\vec{q}l}^{(\lambda)}\| = \frac{1}{i\hbar} \begin{bmatrix} 2\hat{B}_{\vec{q}l}^{(\lambda)} \hat{\sigma}_l^- \\ -2\hat{B}_{\vec{q}l}^{(\lambda)} \hat{\sigma}_l^+ \\ 0 \end{bmatrix} \quad (51)$$

Here  $\hat{B}_{\vec{q}l}^{(\lambda)}$  is

$$\hat{B}_{\vec{q}l}^{(\lambda)} = \sum_{\vec{q}} \lambda_{\vec{q}l} (\hat{b}_{\vec{q}}^+ + \hat{b}_{\vec{q}}), \quad (52)$$

$\hat{b}_{\vec{q}}^+$  ( $\hat{b}_{\vec{q}}$ ) is the creation (annihilation) operator of the phonon with impulse  $\vec{q}$  and with energy  $\hbar\omega_{\vec{q}}$ ,  $\lambda_{\vec{q}l}$  is electron-phonon coupling constant. In equations (41) and (42)  $\|\sigma_P^z\|$  is Pauli  $z$ -matrix,  $\|g\|$  in equation (40) is diagonal matrix, numerical values of its elements are dependent on the basis choice. It is at appropriate basis

$$\|g\| = \begin{bmatrix} 1 & 0 & 0 \\ 0 & 1 & 0 \\ 0 & 0 & 1 \end{bmatrix}. \quad (53)$$

Right hand side expression in (46) is vector product of vector operators. It can be calculated in accordance with expression

$$\left[ \hat{\sigma}_l \otimes \hat{\mathcal{G}}_{l-1,l+1} \right] = \frac{1}{2} \begin{vmatrix} \vec{e}_- \times \vec{e}_z & \hat{\sigma}_l^- & \hat{\mathcal{G}}_{l-1,l+1}^- \\ \vec{e}_z \times \vec{e}_+ & \hat{\sigma}_l^+ & \hat{\mathcal{G}}_{l-1,l+1}^+ \\ \vec{e}_+ \times \vec{e}_- & \hat{\sigma}_l^z & \hat{\mathcal{G}}_{l-1,l+1}^z \end{vmatrix}', \quad (54)$$

that is by using of known expression for usual vector product with additional coefficient  $\frac{1}{2}$  the only, which is appeared, since the products of two components of two vector operators are replaced by anticommutators of corresponding components. Given detail is mapped by symbol  $\otimes$  in (46) and by symbol  $'$  in determinant (54).

It follows from comparison with semiclassical Landau-Lifshitz (L-L) equation for dynamics of spectroscopic transitions for a chain of exchange coupled centers [46], [44], that the equation, which is given by (40) is its QED-generalization. In comparison with semiclassical description, where for the description of dynamics of spectroscopic transitions is sufficient the only one vector equation (L-L equation or L-L based equation), in the case of completely quantum consideration L-L type equation describes the only one subsystem of three-part-system, which consist of EM-field, dipole moments' (magnetic or electric) matter subsystem and phonon subsystem. It was concluded in [44], that the presence of additional equations for description of transition dynamics by QED model in comparison with semiclassical model leads to a number of new effects, which can be predicted the only by QED consideration of resonance transition phenomena.

The terms like to right hand side terms in (42) were used in so called "spin-boson" Hamiltonian [47] and in so called "independent boson model" [48]. Given models were used to study phonon effects in a single quantum dot within a microcavity [49], [50], [51], [52], [53]. So, it has been shown in [52], [53], that the presence of the term in Hamiltonian [44]

$$\hat{\mathcal{H}}^{CPH} = \sum_{j=1}^N \sum_{\vec{q}} \lambda_{\vec{q}} (\hat{b}_{\vec{q}}^+ + \hat{b}_{\vec{q}}) \hat{\sigma}_j^z, \quad (55)$$

which coincides with corresponding term in Hamiltonian in [52], [53] at  $N = 1$  [contribution of given term to the equations for spectroscopic transitions is  $\pm \sum_{l=1}^N \hat{\sigma}_l^z \lambda_{\vec{q}}$ ,

see equation (42), (note that the equations for spectroscopic transitions were not derived in above cited works [49], [50], [51], [52], [53]) leads the only to exponential decrease of the magnitude of quantum Rabi oscillations with increase of electron-phonon coupling strength and even to their suppression at relatively strong electron-phonon coupling. However, it is shown in [43], that by strong electron-photon coupling and strong electron-phonon coupling quite other picture of quantum relaxation processes becomes to be possible. It is argued in given work the following. The definition of the wave function of the chain system, interacting with quantized EM-field and with quantized lattice vibration field, to be vector of the state in Hilbert space over quaternion ring, that is quaternion function of quaternion argument, leads to Lorentz invariance of the equations (40) to (42) and to possibility of the transfer to observables. In fact, in the work cited, the main role of spin vector for the quantum state description was taken into account. Since spin vector is vector of the state [in Hilbert space over quaternion ring with accuracy to normalization factor] of 1D quantum system, interacting with quantized electromagnetic field, all the components of the vector of the state, that is the components of spin vector, being to be peer components, have to be taken into consideration. At the same time, the Hamiltonian, given by (55) describes in fact the only part of interaction with phonon field, which corresponds the only to  $z$ -component of the vector of the state. The interaction of dipole subsystem with phonon field, corresponding to  $x$ - and  $y$ -components of the vector of the state of dipole subsystem (that is,  $S^+$ - and  $S^-$ -components of the spin of matter subsystem, since they are proportional to two linear combinations of peer  $x$ - and  $y$ -components of vector of the state of the system considered) was taken into consideration in [43]. Therefore, the following Hamiltonian was obtained in a natural way

$$\hat{\mathcal{H}} = \hat{\mathcal{H}}^C + \hat{\mathcal{H}}^F + \hat{\mathcal{H}}^{CF} + \hat{\mathcal{H}}^{Ph} + \hat{\mathcal{H}}^{CPH}, \quad (56)$$

where  $\hat{\mathcal{H}}^C$  is chain Hamiltonian by the absence of the interaction with EM-field,  $\hat{\mathcal{H}}^F$  and  $\hat{\mathcal{H}}^{Ph}$  are photon and phonon field Hamiltonians correspondingly,  $\hat{\mathcal{H}}^{CF}$  and  $\hat{\mathcal{H}}^{CPH}$  are, accordingly, Hamiltonians, describing the interaction between quantized EM-field and electronic subsystem of atomic chain and between quantized phonon field and electronic subsystem of atomic chain. Then the equations of the motion for spectroscopic transition operators  $\hat{\sigma}_l$ , for quantized EM-field operators  $\hat{a}_{\vec{k}}$ ,  $\hat{a}_{\vec{k}}^+$  and for phonon field operators  $\hat{b}_{\vec{q}}$ ,  $\hat{b}_{\vec{q}}^+$  are the following. Instead equation (40) the equation

$$\frac{\partial}{\partial t} \begin{bmatrix} \hat{\sigma}_l^- \\ \hat{\sigma}_l^+ \\ \hat{\sigma}_l^z \end{bmatrix} = 2 \|g\| \begin{bmatrix} \hat{F}_l^- \\ \hat{F}_l^+ \\ \hat{F}_l^z \end{bmatrix} + \|\hat{R}_{\vec{q}l}^{(\lambda^z)}\| + \|\hat{R}_{\vec{q}l}^{(\lambda^\pm)}\| \quad (57)$$

takes place, where matrix  $||\hat{R}_{\vec{q}l}^{(\lambda^z)}||$  is

$$||\hat{R}_{\vec{q}l}^{(\lambda^z)}|| = \frac{1}{i\hbar} \begin{bmatrix} 2\hat{B}_{\vec{q}l}^{(\lambda^z)}\hat{\sigma}_l^- \\ -2\hat{B}_{\vec{q}l}^{(\lambda^z)}\hat{\sigma}_l^+ \\ 0 \end{bmatrix} \quad (58)$$

with  $\hat{B}_{\vec{q}l}^{(\lambda^z)}$ , which is given by

$$\hat{B}_{\vec{q}l}^{(\lambda^z)} = \sum_{\vec{q}} [(\lambda_{\vec{q}l}^z)^* \hat{b}_{\vec{q}}^+ + \lambda_{\vec{q}l}^z \hat{b}_{\vec{q}}]. \quad (59)$$

Matrix  $||\hat{R}_{\vec{q}l}^{(\lambda^\pm)}||$  is

$$||\hat{R}_{\vec{q}l}^{(\lambda^\pm)}|| = \frac{1}{i\hbar} \begin{bmatrix} -\hat{B}_{\vec{q}l}^{(\lambda^\pm)}\hat{\sigma}_l^z \\ \hat{B}_{\vec{q}l}^{(\lambda^\pm)}\hat{\sigma}_l^z \\ \hat{B}_{\vec{q}l}^{(\lambda^\pm)}(\hat{\sigma}_l^+ - \hat{\sigma}_l^-) \end{bmatrix}, \quad (60)$$

where  $\hat{B}_{\vec{q}l}^{(\lambda^\pm)}$  is

$$\hat{B}_{\vec{q}l}^{(\lambda^\pm)} = \sum_{\vec{q}} [(\lambda_{\vec{q}l}^\pm)^* \hat{b}_{\vec{q}}^+ + \lambda_{\vec{q}l}^\pm \hat{b}_{\vec{q}}]. \quad (61)$$

The equation (41) remains without changes. The equation (42) is

$$\begin{aligned} \frac{\partial}{\partial t} \begin{bmatrix} \hat{b}_{\vec{k}} \\ \hat{b}_{\vec{q}}^+ \end{bmatrix} &= -i\omega_{\vec{q}} ||\sigma_P^z|| \begin{bmatrix} \hat{b}_{\vec{q}} \\ \hat{b}_{\vec{q}}^+ \end{bmatrix} + \\ \frac{i}{\hbar} \begin{bmatrix} -\sum_{l=1}^N \{ \lambda_{\vec{q}l}^z \hat{\sigma}_l^z + \lambda_{\vec{q}l}^\pm (\hat{\sigma}_l^+ + \hat{\sigma}_l^-) \} \\ \sum_{l=1}^N \{ \lambda_{\vec{q}l}^z \hat{\sigma}_l^z + \lambda_{\vec{q}l}^\pm (\hat{\sigma}_l^+ + \hat{\sigma}_l^-) \} \end{bmatrix}. \end{aligned} \quad (62)$$

Here  $\lambda_{\vec{q}}^z$  and  $\lambda_{\vec{q}}^\pm$  are electron-phonon coupling constants, which characterise respectively the interaction of electron subsystem of  $j$ th chain unit, corresponding to  $z$ -component of its vector of state (or  $S_j^z$ ) and the interaction of electron subsystem of  $j$ th chain unit, corresponding to  $\pm$ -components of its vector of state (or  $S_j^+$ - and  $S_j^-$  components of the spin of  $j$ th chain unit). It seems to be understandable, that they can be different in general case. Moreover, in order to take into account the interaction with both equilibrium and nonequilibrium phonons both the electron-phonon coupling constants have to be complex numbers.

Thus, QFT model for dynamics of spectroscopic transitions in 1D multiqubit exchange coupled system was generalized by taking into account, that spin vector is proportional to quaternion vector of the state of any

quantum system in Hilbert space defined over quaternion ring and consequently all the spin components has to be taken into account. New quantum phenomenon was predicted in [43]. The prediction results from the structure of the equations derived and it consists in the following. The coherent system of the resonance phonons, that is, the phonons with the energy, equaled to resonance photon energy can be formed by resonance, that can lead to appearance along with Rabi oscillations determined by spin (electron)-photon coupling with the frequency  $\Omega^{RF}$  of Rabi oscillations determined by spin (electron)-phonon coupling with the frequency  $\Omega^{RPh}$ . In other words, QFT model predicts the oscillation character of quantum relaxation, that is quite different character in comparison with phenomenological and semiclassical Bloch models. Moreover, if  $|\lambda_{\vec{q}}^\pm| < g$  the second Rabi oscillation process will be observed by stationary state of two subsystems {EM-field + magnetic (electric) dipoles}, that is, it will be registered in quadrature with the first Rabi oscillation process. It can be experimentally detected even by stationary spectroscopy methods.

The second quantum Rabi oscillation process is governed by the formation of the coherent system of the resonance phonons. Therefore along with absorption process of EM-field energy the coherent emission process can take place. Both the quantum Rabi oscillation processes can be time-shared. For the case of radiospectroscopy it corresponds to the possibility of the simultaneous observation along with (para)magnetic spin resonance the acoustic spin resonance.

The predicted phenomenon of the formation of the coherent system of the resonance phonons can find the number of practical applications, in particular it can be used by elaboration of various logic quantum systems including quantum computers and quantum communication systems. The appearance of coherent system of the resonance hypersound phonons with high energy seems to be crucial for the switch of electronic system of NTs to AFM-SSt. Really, let us consider the most simple example BCS s-wave mechanism of superconductivity. It is taking place, when the interaction between electrons, realised through phonon subsystem, will be attractive. In its turn, given interaction is attractive, when the energy difference between the electron states involved is less than phonon energy  $\hbar\omega_{ph}$  [24]. In other words, the most significant contribution to the attractive interaction energy is given by short-wavelength phonons.

Therefore, the appearance of coherent system of high energy hypersound phonons in resonance conditions seems to be having key role for switch of the NTs-network in the sample studied to the state, characterised by superconductivity and uncompensated antiferromagnetism. On the other hand, it is strong argument, that phonon-mediated mechanisms are also give contribution to total superconducting state.

Let us remark, that there are additional results in favour of model proposed, represented in [36]. The phenomenon of ferrimagnetic spin wave resonance [un-

compensated antiferromagnetic spin wave resonance] has been established [for the first time in magnetic resonance spectroscopy] by more detailed analysis of the spectra observed. The fact itself of observation of uncompensated antiferromagnetic spin wave resonance (SWR) is direct proof of the formation of antiferromagnetic ordering [uncompensated]. Spin wave resonance observed has two main peculiarities.

1. The opposite deviation of the asymmetry extent ratio  $A/B$  from 1 of resonance modes in comparison with main AFM mode, at that given deviation increases with mode number increase. It is the result, which allows to exclude from the consideration the Dyson effect. Given peculiarity of ferrimagnetic spin wave resonance was explained qualitatively by existence of nodes like to explanation of the asymmetry extent of the resonance lines in a  $d_{x^2-y^2}$  superconductors.

2. The substantial increase of the intensity of ferrimagnetic spin wave resonance modes with mode number increase. Let us remark, that intensity conservation law for SWR modes was found for NTs incorporated in diamond matrix with other implantation directions [18], carbynes and for some organic quasi-1D substances (polyvinylidenehalogenides - PVDF) [21]. In the other earlier known cases, for instance, by SWR in ferromagnetic metals, the intensity of SWR modes is decreasing with mode number increasing, see, for example, Figure 1 in [54]. The peculiarity observed in the sample studied is explained by taking into account the presence of the magnetic fluctuation spectrum consisting of the continuum of the AFM spin fluctuations peaked at AFM vector  $\vec{Q}$ . For SWR modes wave vector  $|\vec{q}| \neq 0$  and  $|\vec{q}|$  is increasing with mode number increase, coming near to the value of  $\vec{Q}$ . Then the dynamical magnetization will be determined by Fourier component of the magnetic fluctuation field with the frequency, coinciding with the operating microwave frequency of the spectrometer. Given component is added to dynamical magnetization produced by magnetic component of microwave field used and it determines mode intensity growth with unusual asymmetry extent.

The observation of the only peculiarities of SWR above indicated seems to be sufficient to insist on the formation in NTs' network of the sample studied of  $s^+$ -superconductivity at room temperature, coexisting with uncompensated antiferromagnetic ordering.

The results above discussed can be considered to be the basis for the method of identification of superconducting states, coexisting with magnetism.

## V. CONCLUSIONS

The formation in carbon NTs, produced by high energy ion beam modification of diamond single crystals in  $\langle 100 \rangle$  direction and representing themselves the surface of ion tracks, of uncompensated antiferromagnetic ordering coexisting with superconductivity at room tempera-

ture is argued. It is based on ESR studies. A number of peculiarities has been observed for the first time in radiospectroscopy. They are the following.

1. It is the fact itself of the switch in resonance conditions to other rather stable state. It was shown, that new state is defined by uncompensated antiferromagnetic ordering coexisting with superconductivity. It is characterised spectroscopically by appearance of two new rather broad anisotropic lines, designated L and  $R_b$ , which have, however, quite different spectroscopic properties, and by two very broad intensive lines.

2. Dependence of absorption amplitude of the right broad line  $R_b$  in ESR spectrum of NTs on magnetic component of microwave field is strongly nonlinear. It is characterised for the values of relative magnetic component of microwave field  $H_1/H_1^{(0)}$  in the range (0-0.75) by usual saturating law, but in the range (0.75-1) it acquires prominent superlinear nonsaturating character.

3. Unusual angular dependence of asymmetry extent, which cannot be described within the framework of Dyson theory.

Main details in very pronounced angular dependencies of linewidth of the left line L and intensity of absorption, corresponding to given line are explained by corresponding angular dependence of Meissner effect. It has been showed, that broadening mechanism, determined by Meissner effect, will take place for any paramagnetic, or magnetically ordered system, localised in superconducting region, that is, given broadening mechanism is universal. It is established for the first time in radiospectroscopy.

Penetration depth of static magnetic field was evaluated to be equal  $\approx 34$  nm.

Difference in linewidths of the line L and  $R_b$  is analysed within the frames of relaxation theory in superconducting state (SSt), which takes into account the anomalous density of states (DOS) originating from the coherence effect of the transition probability in the SSt. DOS, originating from the coherence effect gives rise to linewidth of the line L, which is responsible for  $s^+$  branch of mixed  $s^+p$ -wave superconductivity. At the same time, in  $p$ -wave SSt the coherence effect is cancelled out by integrating over the momentum space on the SSt-gap, that is, it does not give rise to linewidth of the line  $R_b$ , which is responsible for  $p$  branch.

Hamiltonian for mathematical description of the phenomenon observed is built. It is based on the concept of 1D Fermi liquid for electronic states of quasi-1D systems, the concept was developed earlier, however, it is shortly reviewed in given paper.

The analysis of the concept of 1D Fermi liquid allowed to propose a number of the other possible mechanisms of SSt formation in the sample studied. On the one hand,  $s$ -wave mechanism, mediated by the coupling of charge carriers with stretched phonon modes like to  $MgB_2$ , heavily boron doped diamond and sandwich S-Si-QW-S structures can be taking place. Moreover, just crimped cylindrical shape of NTs allows to increase the strength of

C-C bonds by preservation of high density of the states on FS, resulting from low dimensionality. On the other hand, the multiband structure of valence and conductivity bands allows to realise the formation of AFM-SSt by means of the  $s^+$ -wave formation like to pnictides and additionally  $p$ -wave formation. It seems to be new mechanism - joint  $s^+$ - $p$ -wave mechanism. Just given mechanism is experimentally proved. The independent on dimerization coordinate electron-electron repulsion terms in the Hamiltonian proposed can give the contribution to AFM-SSt formation by given mechanism. The foregoing theoretical consideration allow to suggest also, that usual s-wave BCS mechanism with  $S = 0$  Cooper pairing process of quasiparticles can produce additional independent superconducting channel. Given mechanism cannot be detected, however, by magnetic resonance technique directly. Along with given mechanism, the s-wave BCS-like mechanism with  $S = 1$  Cooper pairing process of quasiparticles can in principle also take place. The attractive terms Hamiltonian, which are proportional to dimerization coordinate, can contribute to given phonon-mediated mechanisms and to s-wave mechanisms, mediated by the coupling of charge carriers with stretched phonon modes like to those ones established in  $MgB_2$ ,

heavily boron doped diamond and sandwich S-Si-QW-S structures. Further, the formation of  $\sigma$ -polaron lattice with AFM-ordering, which can take place in the NTs, leads to new possible mechanism of AFM-SSt formation. It will be pure  $s^+$ -wave mechanism, like to those taking place in many pnictides. Main feature, which differ given mechanism from known ones is the other spatial distribution of delocalized spins. It is  $\sigma$ -polaron lattice instead spin density wave.

Especially interesting seems to be the role of external quantized EM-field, which proposed to be responsible for the switch to SSt by means of formation of coherent long-lived systems of resonance hypersound phonons. The corresponding quantum field theory was proposed something earlier, however, brief review is given. Based on given result, we can conclude, that quantized radiospectroscopy-range EM-field seems to be working constituent for realization of room temperature SSt. On the other hand, it is considered to be strong argument of the participation in the SSt-formation of BCS or BCS-like mechanisms (maybe the only at the stage of a transitional process). Thus, the room temperature SSt in  $\langle 100 \rangle$ -NTs, incorporated in diamond matrix can be formed in the result of participation of several mechanisms.

- 
- [1] Nagamitsu J., Nakagawa N., Muranaka T., and Akimitsu J., *Nature*, **410** (2001) 63
  - [2] An J M and Pickett W E, *Phys.Rev.Lett.*, **86** (2001) 4366
  - [3] Kortus et al., *Phys.Rev.Lett.*, **86** (2001) 4656
  - [4] Kong Y. et al., *Phys.Rev.B*, **64** (2001) 020501
  - [5] Ekimov E A, Sidorov V A, Bauer E D, Mel'nik N N, Curro N J, Thompson J D, and Stishov S M, *Nature*, **428** (2004) 542
  - [6] Takano Y., Nagao M., Kobayashi K., Umezawa H., Sakaguchi I., Tachiki M., Hatano T., and Kawarada H., *Appl.Phys.Lett.*, **85** (2004) 2581
  - [7] Blase X, Adessi Ch, Connetable D, *Phys.Rev.Lett.*, **93** (2004) 237004
  - [8] Lee K.-W. and Pickett W E, *Phys.Rev.Lett.*, **93** (2004) 237003
  - [9] Kawaji H., Horie H.-O., Yamanaka S., and Ishikawa M., *Phys.Rev.Lett.*, **74** (1995) 1427
  - [10] Bagraev N T, Gehlhoff W, Klyachkin L E, Malyarenko A M, and Romanov V V, arXiv:0806.2800v1 [cond-mat.supr-con]
  - [11] Kamihara Y., Watanabe T., Hirano M., and Hosono H., *J.Am.Chem.Soc.*, **130** (2008) 3296
  - [12] Chubukov A V, Efremov D V, and Eremin I, *Phys.Rev.B*, **78** (2008) 134512-134512-10
  - [13] Erchak D.P, Penina N.M, Stelmakh V.F, Tolstykh VP, Zaitsev AM, The 7th Int.Conf.IBMM 90, Abstracts, Knoxville, USA, 1990, p.313
  - [14] Efimov V.G, Erchak D.P, Gelfand R.B, Penina N.M, Stelmakh V.F, VS Varichenko, Ulyashin A.G, Zaitsev AM, EMRS 1990 Fall Meeting, Abstracts, Strasbourg, France, 1990, p.C-V/P 12
  - [15] Kawataba K., Mizutani M., Fukuda M., Mizogami S., *Synthetic Metals*, **33** (1989) 399-402
  - [16] Erchak D.P, Efimov V.G, Zaitsev AM, Stelmakh V.F, Penina N.M, Varichenko VS, Tolstykh VP, *Nucl.Instrum.Meth.in Phys.Res.,B*, **69** (1992) 443-451
  - [17] Erchak D.P, Guseva M.B, Alexandrov A.F, Alexander H, Pilar v.Pilchau A, Pis'ma Zh.Experiment.Teor.Fiz., **58**, N 4 (1993) 268-271, *JETP Letters*, **58**, N 4 (1993) 275-278
  - [18] Ertchak D.P, Efimov V.G, Stelmakh V.F, Review, *Zh.Prikladn.Spectr.*, **64**, N 4 (1997) 421-449, *J.Appl.Spectr.*, **64**, N 4, (1997) 433-460
  - [19] Ertchak D.P, Efimov V.G, Stelmakh V.F, Martinovich V.A, Alexandrov A.F, Guseva M B, Penina N.M, Karpovich I.A, Varichenko V S, Zaitsev A M, Fahrner W R, Fink D, *Phys.Stat.Sol.,b*, **203**, N2 (1997) 529-548
  - [20] Yerchuck D, Dovlatova A, *J.Phys.Chem.,C*, DOI: 10.1021/jp205549b, **116**, N 1 (2012) 63-80
  - [21] Yearchuck D, Yerchak Y, Alexandrov A, *Phys.Lett.A*, **373**, N 4 (2009) 489-495
  - [22] Dovlatova A, Yearchuck D, *Chem.Phys.Lett.*, **511** (2011) 151-155
  - [23] Dmitri Yerchuck, Vyacheslav Stelmakh, Alla Dovlatova, Yauhen Yerchak, Andrey Alexandrov, in press
  - [24] Bardeen J, Cooper L N, Schrieffer J.R, *Phys.Rev.*, **108**, N 5 (1957) 1175-1204
  - [25] Dyson F D *Phys.Rev.* **98** (1955) 349-359
  - [26] Erchak D.P, Zaitsev A M, Stel'makh V.F, Tkachev V D, *Phys.Tekhn.Polupr.*, **14**, N 1 (1980) 139-143, *Sov.Phys.Semicond.*, USA, **14**, N 1 (1980) 79-82
  - [27] Poole C P, Jr, *Technique of EPR-spectroscopy*, Moscow, Mir, 1970, 557 pp
  - [28] Tomonaga S., *Prog.Theor.Phys.*, **5** (1950) 544
  - [29] Luttinger J M, *J.Math.Phys.*, **4** (1963) 1154
  - [30] Alla Dovlatova, Dmitri Yerchuck, Felix Borovik, in press



- [31] Su W.P., Schrieffer J.R, and Heeger A.J, Phys.Rev.Lett., **42** 1698 (1979)
- [32] Su W.P., Schrieffer J.R, and Heeger A.J, Phys.Rev.B, **22**, (1980) 2099
- [33] Lifshitz E.M, Pitaevsky L.P, Statistical Physics, part 2, M., Nauka, 1978, 448 pp
- [34] Heeger A.J, Kivelson S, Schrieffer J.R, Su W.-P., Rev.Mod.Phys., **60** (1988) 781-850
- [35] Kittel C, Phys.Rev., **82** (1951) 565
- [36] Dmitri Yerchuck, Yauhen Yerchak, Vyacheslav Stelmakh, Alla Dovlatova, Andrey Alexandrov, in press
- [37] Zhang J, Sknepnek R and Schmalian J, Phys.Rev.B, **82** (2010) 134527
- [38] Korshunov M.M, Eremin I, Phys.Rev.B, **78** (2008) 140509(R)
- [39] Rao S S, Stesmans A, Noyen J V, Jacobs P, Sels B, Europhys.Lett., **90**, N 5 2010 57003
- [40] Wallace P R, Phys.Rev., **71** (1947) 622-634
- [41] Castro Neto A H, Guinea F, Peres N M R, Novoselov K S, and Geim A K, Rev.Mod.Phys., **81** (2009) 109
- [42] Hidekazu Mukuda, Mariko Nitta, Mitsuharu Yashima, Yoshio Kitaoka, Parasharam M. Shirage, Hiroshi Eisaki, and Akira Iyo, J.Phys.Soc.Jpn, **79** N 11 (2010) 113701/1-4 DOI: 10.1143/JPSJ.79.113701
- [43] Alla Dovlatova and Dmitri Yerchuck, ISRN Optics, Article ID 390749, 10 pp (2012) doi:10.5402/2012/390749
- [44] D.Yearchuck, Y.Yerchak, A.Dovlatova, Optics Communications, **283** (2010) 3448-3458
- [45] Tavis M, Cummings F W, Phys.Rev., **170**(2) (1968) 387
- [46] Yearchuck D, Yerchak Y, Red'kov V, Doklady NANB, **51** (2007) 57-64
- [47] Leggett A J, Chakravarty S Chakravarty, Dorsey A T, Fisher M P A et al, **59** (1987) 1
- [48] Mahan G D, Many-Particle Physics, Plenum, New York, 2000
- [49] Heitz R, Mukhametzhanov I, Stier O, Madhukar A, and Bimberg D, Phys.Rev.Lett., **83** 1999 4654
- [50] Türck V, Rodt S, Stier O et al, Phys.Rev.B, **61**, (2000) 9944
- [51] Besombes L, Kheng K, Marsal L, and Mariette H, Phys.Rev.B, **63** (2001) 155307
- [52] Wilson-Rae I and Imamoglu A, Phys.Rev., B **65** (2002) 23531
- [53] Ka-Di Zhu, Zhuo-Jie Wu, Xiao-Zhong Yuan, and Hang Zheng, Phys.Rev.B, **71** (2005) 235312
- [54] Seavey M H, Jr, Tannenwald P E, Phys.Rev.Lett., **1**, N 5 (1958) 168-170